THE UNIVERSITY OF ALBERTA

ANALYSIS AND SIMULATION OF PARTICLE MOTION ON OSCILLATING SCREENS

by

JINGLU TAN

A THESIS

SUBMITTED TO THE FACULTY OF GRADUATE STUDIES AND RESEARCH

IN PARTIAL FULFILMENT OF THE REQUIREMENTS FOR THE DEGREE

OF MASTER OF SCIENCE

IN

AGRICULTURAL ENGINEERING

DEPARTMENT OF AGRICULTURAL ENGINEERING

EDMONTON, ALBERTA

Spring, 1986

ISBN 0-315-30231-3

THE UNIVERSITY OF ALBERTA

RELEASE FORM

NAME OF AUTHOR JINGLU TAN

TITLE OF THESIS ANALYSIS AND SIMULATION OF PARTICLE MOTION ON OSCILLATING SCREENS

DEGREE FOR WHICH THESIS WAS PRESENTED MASTER OF SCIENCE

YEAR THIS DEGREE GRANTED Spring, 1986

(SIGNED) ..[illegible]..........

PERMANENT ADDRESS:

..[illegible]...

....[illegible]........

..Shandong, China........

DATED ..March 28.....1986

THE UNIVERSITY OF ALBERTA

FACULTY OF GRADUATE STUDIES AND RESEARCH

The undersigned certify that they have read, and recommend to the Faculty of Graduate Studies and Research, for acceptance, a thesis entitled ANALYSIS AND SIMULATION OF PARTICLE MOTION ON OSCILLATING SCREENS submitted by Jinglu Tan in partial fulfilment of the requirements for the degree of MASTER OF SCIENCE in Agricultural Engineering.

....
Supervisor

....

....

Date....3/19/86....................

ABSTRACT

The effectiveness of oscillating screens is affected by a number of factors, which include the frequency and the amplitude of oscillation, the screen slope and the drive type etc. To investigate the ways of improving the screening effectiveness, the study examined the the effect of four different drives; that is, the crank-pitman, the bent-shaft and the quick-return oscillators, and the spatial crank slider. The effect of the other variables was also evaluated when each of the four drives was used.

The kinematic equations describing the motion of the screen with each of the four drives were derived by using the relative motion theories; and the dynamic state of a particle moving on the screen was analysed when the particle was limited to continuous sliding motion. The dependent variables, which indicate the screening effectiveness, are defined. The dependent variables are the average relative velocity, the penetrating ratio and the efficiency index. On the basis of the dynamic and kinematic analyses, a computational model was developed with all the independent variables as parameters. The model was run for each of the four drives and different combinations of the independent variables. The result data were plotted or tabulated.

The significant factors affecting the motion of the particle are the frequency and the amplitude of oscillation, and the screen slope. The frequency and the amplitude have much the same effects on particle motion; the screening effectiveness increases with either of them to a maximum and then decreases. The effect of increasing the screen slope depends on the frequency and the amplitude used. The crank-pitman oscillator and the spatial crank slider impart very similar motion to the screen and the particle and they give a better opportunity for particle penetration than the other two drives. Compared with the other drives, the quick-return drive can substantially increase the percentage of the time when the particle velocity relative to the screen is lower than limit velocities. A motion with low maximum acceleration is not desirable for effective screening.

ACKNOWLEDGEMENT

The auther would like to acknowledge the moral support of his fimily and the patient guidance of Dr. H. P. Harrison for this project.

TABLE OF CONTENTS

LIST OF TABLES

LIST OF FIGURES

1. INTRODUCTION

Screening of particulate materials is a very important process in both agriculture and industry. In agriculture, grains are separated from contaminants through screening; and seeds are usually cleaned and graded by way of screening before they are sown. In milling and brewing industries, thousands of tons of grains are cleaned and graded every day. Besides, many other areas, such as medical drug production and construction material production, also involve a great deal of screening of particulate materials.

Though many different types of machines are used, the most commonly used equipment to accomplish screening is an oscillating screen. The effectiveness of the oscillating screen is affected by a number of variables, which include the frequency and the amplitude of oscillation, the screen slope and the drive type. In view of the practical importance of the screening process, the determination of the best operating conditions for the oscillating screen is obviously essential.

The research work done so far (Garvie 1966, Feller and Foux 1975, Harrison and Blecha 1983) on oscillating screens has shown the following:

(a) the magnitude of the maximum acceleration of the screen is a major factor affecting the screening efficiency, and there is an optimum value that gives the highest efficiency.

(b) there is a limit to the particle velocity relative to the screen beyond which the particle cannot penetrate the screen perforations; and the percentage of the time when the relative velocity exceeds the limit velocity indicates the opportunity that an oscillating screen can provide for the passage of the particle through perforations.

(c) controlling the orientation of prolate spheroid particles can improve the precision of separation of such particles from those having a spherical shape.

In all the previous work mentioned above, the crank-pitman oscillator has been exclusively used as the drive of the screen, and moreover, the screen motion has been assumed to be sinusoidal in most cases, which may have greatly limited the scope and the precision of the research work. Harrison and Blecha (1983) states that the use of a quick-return screen motion could be beneficial. As a result it is necessary that different drives, therefore different screen motions be tried, and the effects of the other factors be further evaluated.

2. LITERATURE REVIEW

2.1 Oscillating Screens and Conveyors

An oscillating screen or an oscillating conveyor is essentially a surface supported or mounted on parallel links forming a parallelogram four-bar link mechanism which is actuated by a reciprocating drive such as a crank-pitman oscillator. Fig. 1 shows a typical oscillating screen or conveyor with a the crank-pitman drive.

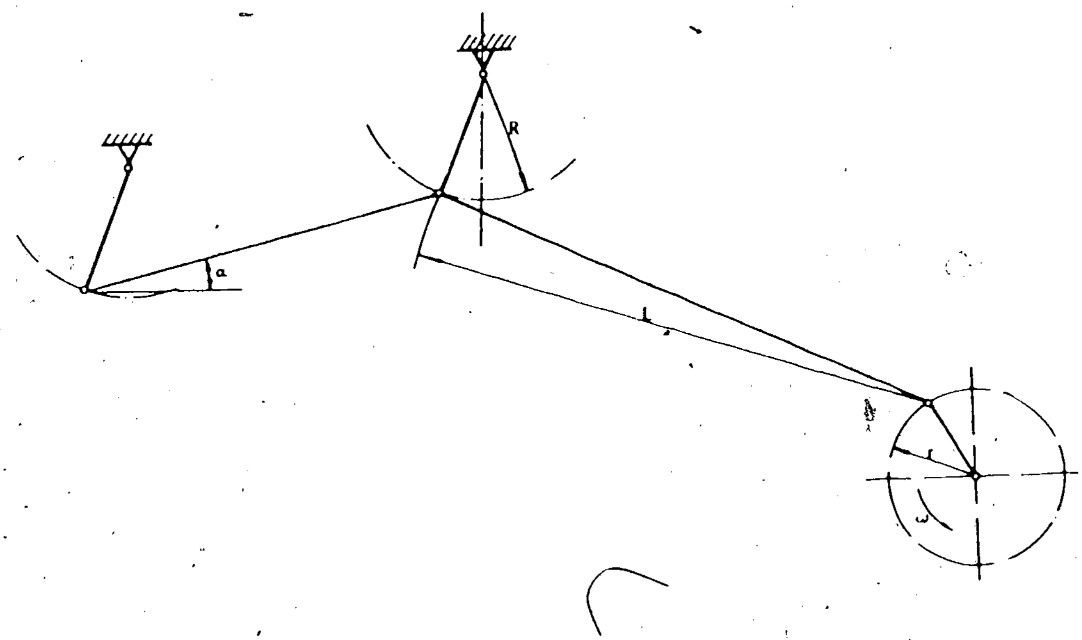

Fig. 1 The Schematic of an Oscillating Screen or Conveyor

An oscillating screen can be used to grade or to clean particulate materials. For example, the grain cleaners used on agricultural machinery today are commonly oscillating screens. An oscillating conveyor can transfer particulate materials from one location to another by causing a relative motion between the materials and the conveyor surface.

The major structural difference between the oscillating screen and the oscillating conveyor is that the screen surface is perforated whereas the conveyor surface is not; nevertheless, the performances of the oscillating screen and the oscillating conveyor are basically affected by the same group of variables such as the frequency and the amplitude of oscillation, the screen or conveyor slope and the drive type. As a consequence, both screening and conveying have been studied and developed side by side (Berry 1958 & 1959, Schertz and Hazen 1963 & 1965, Garvie 1966, Hann and Gentry 1970, Feller and Foux 1975, Harrison and Blecha 1983). The theories and results obtained on one of them can be referenced and even used on the other. Feller and Foux (1975) observed the motion of a corn seed on both perforated and non-perforated surfaces. They noticed slightly random deviations in particle displacement and smaller average relative displacement on perforated surfaces; however, the general characteristics of the particle displacement curves were very similar. They concluded that the equations for determining the particle motion on a non-perforated oscillating surface can be used to determine the particle motion on a perforated oscillating surface, that is, an oscillating screen.

2.2 Motion of Particles

For both the oscillating screen and the oscillating conveyor, how particles move on them is important. In 1958 and 1959, Berry published the first two articles in which he attempted to develop equations for the movement of particles on an oscillating conveyor. He stated that, depending upon the frequency of oscillation, the kinematic state of a rigid particle on an oscillating surface could be in one of the four regimes (Berry 1958):

Regime 1. If the frequency of the pan is sufficiently low the particle will remain stationary with respect to the pan, no sliding whatsoever taking place. The range of frequency over which this motion occurs is given by

$$0 < \omega^2 < \mu_s g/(X_0+Y_0)$$

Where, ω is the frequency,

μ_s is the coefficient of static friction,

g is the acceleration due to gravity,

X_0 is the amplitude of pan oscillation in the direction parallel to the pan surface, and

Y_0 is the amplitude of pan oscillation in the direction vertical to the pan surface.

Regime 2. The frequency is in such a range that the particle slides during part of the cycle and remains stationary to the pan over the rest of the cycle. Berry named this motion stick-slip and the frequency range is given by

$$\mu_s g/(X_0+\mu_s Y_0) < \omega^2 < \mu_s g/(X_0-\mu_s Y_0)$$

Regime 3. The particle is in a continuous sliding motion throughout the cycle, then the frequency will be in the following range.

$$\mu_s g/(X_0-\mu_s Y_0) < \omega^2 < g/Y_0$$

Regime 4. The frequency is great enough so that the particle is partly in contact with the pan surface and sliding, and partly off the pan surface and falling as a free body.

Schertz and Hazen (1963, 1965) studied the motion of granular materials on an oscillating conveyor. They stated that the material could have a combination of four different types of motion. They were (Schertz and Hazen 1961);

(a) free fall,

(b) sliding negatively (down the surface slope),

(c) sliding positively (up the surface slope), and

(d) riding.

They derived the equations for each of the four types of motion and defined the conditions under which each type of motion would end. Then, they simulated the motion of the particle by using the equations and the conditions. To check the validity of the theoretical prediction, they conducted an experiment on a test stand with a plastic specimen as well as with grains. Motion picture photography was employed to observe the particle motion. For some combinations of the frequency, the amplitude, the conveyor slope and frictional coefficient etc. the experimental results showed fairly good agreement with the simulation results, for others they did not.

Following Schertz and Hazen (1963, 1965), Hann and Gentry (1970) did a study with an ellipsoidal object which could roll on the conveyor surface so that the results could be applicable to fruit conveying. They defined that the object could move in one of the following nine modes (Hann and Gentry 1970);

a. roll up normal,
b. roll up reverse,
c. roll down normal,
d. roll down reverse,
e. slide up normal,
f. slide up reverse,
g. slide down normal,
h. slide down reverse, and
i. ride,

where roll means that the object is rolling on the conveyor surface, slide means that the object is both sliding and rolling, up and down mean the up and down conveyor slope directions respectively, and normal and reverse denote whether the rolling velocity is in the same direction as the rolling acceleration or not. From the results of their simulation, they concluded that the average object velocity increases as the amplitude and the frequency of oscillation and the slope angle of the conveyor increase.

Garvie (1966) examined the operating conditions for the maximum effectiveness in grain cleaning and grading. He stated that, to obtain the maximum effectiveness of separation, the continuous sliding of the grain up and down on the screen is the most favorable type of motion since no penetration of the screen perforations is possible while the particle is not in contact with the screen surface.

2.3 Orientation and Natural Rocking Frequency of a Prolate Particle

2.3.1 Orientation

According to Hann and Gentry (1970), a prolate object has a specific orientation when it is supported on an oscillating surface. The orientation can affect the motion of the object on the oscillating surface. The object, when aligned with its long axis parallel to the direction of oscillation, will not travel on an oscillating conveyor if sliding is not induced. It will only rock back and forth. When aligned with its long axis perpendicular to the direction of oscillation, the object will travel normally. The effectiveness of conveying can thus be affected by the orientation. On an oscillating screen the same argument will hold; moreover, the grading accuracy can be affected if the orientation is not taken into account in choosing the size and the shape of perforations.

While studying oscillating conveyors, Hann and Gentry (1970) observed that the orientation of an prolate object is dependent of the frequency of oscillation. When disturbed, a prolate object on a flat level surface will rock at a certain rate. The rate is termed the natural rocking frequency of the object. When the surface oscillates at a frequency higher than the natural rocking frequency of the object, the long axis of the object takes an orientation parallel to the direction of oscillation; when the oscillation frequency is lower than the natural rocking frequency, the long axis takes an orientation perpendicular to the direction of oscillation.

According to Henderson and Newman (1972), a prolate object on an oscillating surface is a slightly damped vibration system. The rocking of the object will be essentially in phase with the surface oscillation when the frequency of surface oscillation is lower than the natural rocking frequency of the object; otherwise the rocking is out of phase. The phase difference affects the direction of the moment caused by the frictional and inertia forces about an axis normal to the surface and the direction of the moment controls the orientation of the object.

2.3.2 Natural Rocking Frequency

When a prolate object is rocking on a flat level surface, its mass center is moving in a vertical plane. If damping is neglected, the rocking is a process of conversion between kinetic energy and potential energy. In other words, the system is conservative or the total energy in the system is a constant; then, the maximum potential energy must equal to the maximum kinetic energy. According to this theory, Mofor (1976) derived an equation for the natural rocking frequency of a prolate object; that is,

$$f = [1/(2\pi)][5g(a^2/b^2-1)]^{1/2}/[b(a^2/b^2+6)]^{1/2},$$

where, a is half of the long axis of the object,

b is half of the short axis of the object,

g is the acceleration due to gravity, and with a, b and g having consistent units.

By using the dimensions of wheat, oats and barley measured by Edison and Brogan (1972), Harrison and Blecha (1983) calculated some natural rocking frequencies with the formula above. As the results were all greater than the oscillating frequencies commonly used on commercial grain cleaners, he concluded that the perpendicular orientation is the usual orientation for grains such as wheat, oats and barley.

2.4 Variables Defining Screen Motion

Berry (1958) defined an oscillating conveyor as a trough or platform which could oscillate in a vertical plane containing the longitudinal axis of the trough (Fig. 1); then, the conveyor is completely specified by (Berry 1958);

a. the mean hanger angle to the vertical,

b. the amplitude of oscillation, and

c. the frequency of oscillation.

Probably, Berry (1958) assumed that the trough was horizontal; however, for oscillating screens, a screen slope angle is often required to transport the oversized particles to the edge of a screen; hence the pan slope should be added as the fourth variable for generality (Feller and Foux 1975, Harrison and Blecha 1983).

The four variables are the main ones which define the geometry of the screen and its motion when a specific driving mechanism is used. Feller and Foux (1975) termed these four variables the screen motion variables.

2.5 Friction between Particles and Screen

In the direction parallel to the screen surface, friction is the only means by which the oscillating screen can exert a force to a particle and causes its state of motion to change; thus, the characteristics of friction (namely kinetic or static), the magnitude and the direction of the frictional force all affect the motion of the particle.

There have been some new theories about the mechanism of friction; however, Coulomb's laws are still widely accepted, especially in engineering areas. Coulomb's laws of friction state that the frictional force (Henderson, 1967);

a. is directly proportional to the normal force acting between two surfaces,

b. is independent of the area of contact,

c. depends on the nature of the materials in contact, and

d. is independent of the relative velocity between the two surfaces in contact when friction is kinetic, i.e., when sliding exists between the surfaces in contact.

Bickert and Buelow (1966) studied the kinetic friction and concluded that the friction coefficients between grains and steel or wood surfaces were not affected by the moisture content, the normal load and the velocity of sliding.

Berry (1959) stated that the kinetic friction coefficient is almost invariably smaller than the static coefficient and that there is no intrinsic relationship between them. It is necessary to determine which coefficient is in effect at a specific time in the process of particle motion. For a particle to slide continuously on an oscillating surface, Feller and Foux (1975) presented the following condition;

$$|d^2X_s/dt^2| \geq |d^2X_p/dt^2| = \mu_k g$$

where, X_s is the displacement of the surface,

X_p is the displacement of the particle,

t is the time,

μ_k is the kinetic coefficient of friction, and

g is the acceleration due to gravity.

If the particle moves up and down on the screen, sliding stops at the instant when the particle velocity relative to the screen changes the direction. Feller and Foux (1975) state that if the equation above holds at that instant, the particle should renew its sliding instantaneously. They also state that It is unnecessary to consider static friction at that instant since the friction does not return immediately to its static value when the sliding ceases.

2.6 Penetration of Particles through Perforations

2.6.1 Conditions for Penetration

Garvie (1966) states that penetration can only occur when the particle is over a perforation and directed through it by means a force, which is normally the force of gravity.

Feller and Foux (1975) state that the screen motion is to facilitate the penetration of particles through perforations; thus, it should satisfy the following requirements;

a. to bring particles into alignment with the perforations,

b. to achieve the appropriate particle velocity relative to the screen for penetration of a particle when it is aligned with a perforation, and

c. to obtain another opportunity for particle penetration if the prior opportunity is unsuccessful.

The first two require that the particle be in motion relative to the screen surface, whereas the second means that the relative velocity, the perforation and the particle sizes should be such that the particle can have enough time to sink into a perforation under the effect of gravity when it is in alignment with the perforation.

2.6.2 Effect of Screen Motion Variables

The penetration of particles through a screen is affected by the screen motion, which in turn is a function of the screen motion variables including the frequency and the amplitude of oscillation, the hanger angle and the screen slope; hence, the influences of these variables on particle penetration are examined.

Garvie (1966) concluded from some early investigations that the effectiveness of a screen depends, to a large extent, on the magnitude of the maximum acceleration of the screen. Feller and Foux (1975) defined the percent of particles that penetrated the screen in a given time period, out of the total number of undersized particles that were loaded on the screen, as the passage percentage. The results of their experiment showed that the passage percentage depended on the maximum screen acceleration as the major parameter. Independently of the effect of the screening duration, the passage percentage increased with the screen acceleration up to a maximum, and then decreased sharply at higher accelerations. They used screen slope angles of up to 10° and hanger angles of up to 30° in their experiment. Either of the two variables showed effect on the passage percentage; consequently, they concluded that the screen inclination and the hanger angle did not affect the penetration of particles at the values common to oscillating screens and that the role of these two variables was limited to the control of screening duration.

2.6.3 Limit Velocity

When a particle is moving on a screen, it can align with a perforation, but it needs time to fall through the perforation under the effect of gravity. In other words, there is a limit to the particle velocity relative to the screen for the particle to pass through a screen perforation of a specific size; above this limit velocity the particle will jump over the perforation rather than pass through it.

For a prolate particle moving down the screen slope as shown in Fig. 2, Garvie (1966) gave the limit velocity as

$$v = [D-(l/2)\cos\alpha]/\{2[(D-l/2)\sin\alpha+(d/2)\cos\alpha]/g\}^{1/2}$$

Where, l is the long axis of the particle,

d is the short axis of the particle,

D is the perforation length, and

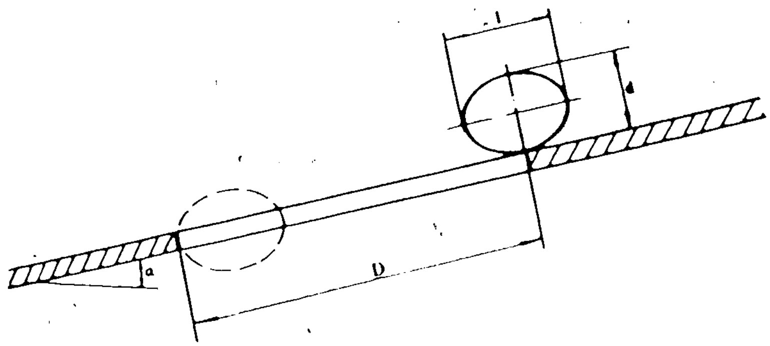

Fig. 2 A Particle Penetrating A Perforation

α is the screen slope angle.

g is the acceleration due to gravity, with the variables having consistent units.

When $\alpha = 0$, that is, for a horizontal oscillating screen,

$$v = (D-1/2)/(d/g)^{1/2}$$

2.7 Driving Mechanisms

A crank-pitman oscillator (see Fig. 1) has been the most commonly used driving mechanism for oscillating screens. Considerably different motion characteristics of the screen can be obtained by changing the dimensions and the relative position between the screen and the drive. Only with some special arrangement can a sinusoidal motion be approximated with the crank-pitman drive; however, a sinusoidal motion of the screen has been assumed by almost all the previous researchers because of the ease of the mathematical description. Turquist and Porterfield (1961) pointed out that this simplifying assumption could affect the validity of the theoretical equations of particle motion on an oscillating surface; moreover, whether driving mechanisms other than the crank-pitman oscillator can improve the screening process has never been attempted. Harrison and Blecha (1983) indicated that a quick-return (non-sinusoidal) screen motion might improve the opportunity of particle penetration without altering the limit velocity. Non-sinusoidal motions can be obtained with some spatial mechanisms and the quick-return mechanism.

2.8 Summary

The oscillating screen and conveyor, though having different functions, are similar in many aspects. Theories developed with one of them can be referenced or adopted for the other.

A particle may move on an oscillating surface in a number of different modes. Depending on the motion of the surface, the particle may slide, roll, slide and roll, ride and even hop on the surface. For an oscillating screen, the desirable type of particle motion is continuous sliding since it gives more chances for the particle to align with screen perforations.

When disturbed, a prolate object on a flat surface rocks at a certain rate, which is termed as the object's natural rocking frequency. This frequency is determined by the geometry of the object only. When the surface is oscillating at a frequency higher than the natural rocking frequency of the object, the object will take the orientation that its long axis is parallel to the plane of oscillation; otherwise perpendicular to the plane. The orientation affects the dimensions of the aperture.

When a specific drive is used, the variables that define the geometry and the motion of an oscillating screen are

a. the frequency of oscillation,

b. the amplitude of oscillation,

c. the screen slope, and

d. the hanger angle.

The major factor affecting the particle penetration is the maximum acceleration of the screen, which is largely determined by the frequency and the amplitude of oscillation. The screen slope and the hanger angle do not affect the particle penetration significantly, but they affect the screening duration.

For specific particle and perforation sizes as well as screen slope, there is a particle velocity relative to the screen known as the limit velocity. When the limit velocity is exceeded, the particle will jump over the perforation without passing through it.

Much of the previous work has been done on oscillating conveyors, and the theory of particle conveying with oscillating conveyors has been comparatively well developed. Harrison and Blecha (1983) has pointed out that very little has been done on oscillating screens. Also, a simple harmonic or sinusoidal motion has been always assumed to avoid the complexity of deriving the exact equations for the screen motion. This assumption can affect the validity of theoretical predictions of particle motion and of the effect of the various variables. Furthermore, whether drives other than the crank-pitman oscillator can improve the screening process has not been studied.

3. OBJECTIVES

The primary objective of the study was to compare the usefulness of different drives to oscillating screens by using the technique of computer simulation. This entailed;

(1) developing equations which describe the motion of the screen when the drive is a;

(a) crank-pitman oscillator,

(b) bent-shaft oscillator,

(c) spatial crank-slider, or

(d) quick-return oscillator.

(2) using the equations to simulate the motion of the particle on an oscillating screen for the following variables;

(a) frequency of oscillation (f),

(b) amplitude of oscillation (A),

(c) screen slope angle (α),

(d) mean hanger angle (ϕ_m),

(e) hanger length (R),

(f) pitman length (L),

and for the crank-pitman drive,

(g) initial pitman slope angle (δ_0),

and for the bent-shaft drive,

(h) bent angle (β),

and for the spatial crank drive,

(i) pitman length of the drive (r_1),

(j) input shaft angle of the drive (β),

and for the quick-return drive,

(k) center distance (h),

(l) swing bar height/center distance ratio (e).

(3) determining which variables are significant to the motion of the particle and which ones are not, and the manner in which the significant variables affect the motion of the particle.

4. MODEL DEVELOPMENT

Modeling is one of the most useful techniques in the theoretical study of physical processes. To simulate the particle motion on an oscillating screen, a computational simulation model was developed. This entailed simplifying the system with some appropriate assumptions and analyzing the motion of the screen and of the particle. The equations determining the velocities and accelerations of the screen were developed for the crank-pitman oscillator, the bent-shaft oscillator, the spatial crank-slider and the quick-return oscillator. The acceleration and velocity of the particle were also determined. The limit velocities were discussed, the penetrating ratio and the efficiency index were defined.

4.1 Assumptions

The following assumptions are made to simplify the system and to develop the simulation model.

(a) Only one particle is assumed to be moving on the screen and it does not contact the side walls of the screen so that there is no particle to particle or particle to side wall interference.

(b) Coulomb's laws of friction apply; i.e., the kinetic coefficient of friction between the particle and the screen surface is constant; and therefore, is independent of the relative velocity and the contact area.

(c) The perforations on the screen do not significantly affect the characteristics of particle motion (Feller and Foux 1975); thus, the effect of screen perforations on particle motion is neglected.

(d) The particle does not roll on the screen as would be the case for some grains.

(e) The length of the screen is ignored.

(f) The air resistance to the moving particle is neglected.

4.2 Motion of the Screen

As noted earlier, the screen surface, the hangers and the frame form a parallelogram four-bar link mechanism (see Fig. 1). The motion of the screen is translational; that is, the kinematic state of every point on it is exactly the same at any time, and the motion of the screen can be represented by that of any single point on it. The joints connecting the hanger and the screen (point S on Fig. 3 is one of them) move along an arc. The length of the arc is the amplitude (A) of the screen motion. The angle between the hanger and the vertical at any time is the hanger angle (ϕ); the hanger angle at an assumed time zero is the initial hanger angle (ϕ_o) and that at the mid-point of the amplitude is refered to as the mean hanger angle (ϕ_m).

The screen can be actuated by several types of reciprocating drives. A crank-pitman oscillator is commonly used because of its simplicity. Other driving mechanisms can also be used though they have not been tried for grain screening. The bent-shaft, the spatial crank-slider and the quick-return are three oscillators that can be used for screen oscillation (Chen 1972). In order to develop the model and compare the effect of different driving mechanisms, the mathematical equations describing the motion of the screen will be herein developed when each of the four drives mentioned above is used.

4.2.1 Oscillating Screen with Crank-pitman Drive

4.2.1.1 Geometric Relationships

The geometric relationships for an oscillating screen with a crank-pitman drive can be examined from Fig. 3 a in which OD is the crank, SD is the pitman or connecting rod and O_1S is a hanger. Suppose that when time t is zero, point D is at D_o; then, as shown by the dotted lines ($O_1S_oD_oO$) in Fig. 3 a, the initial hanger angle is ϕ_o, and the pitman is initially perpendicular to the crank and has an initial slope angle of δ_o. The crank has a length of r and is

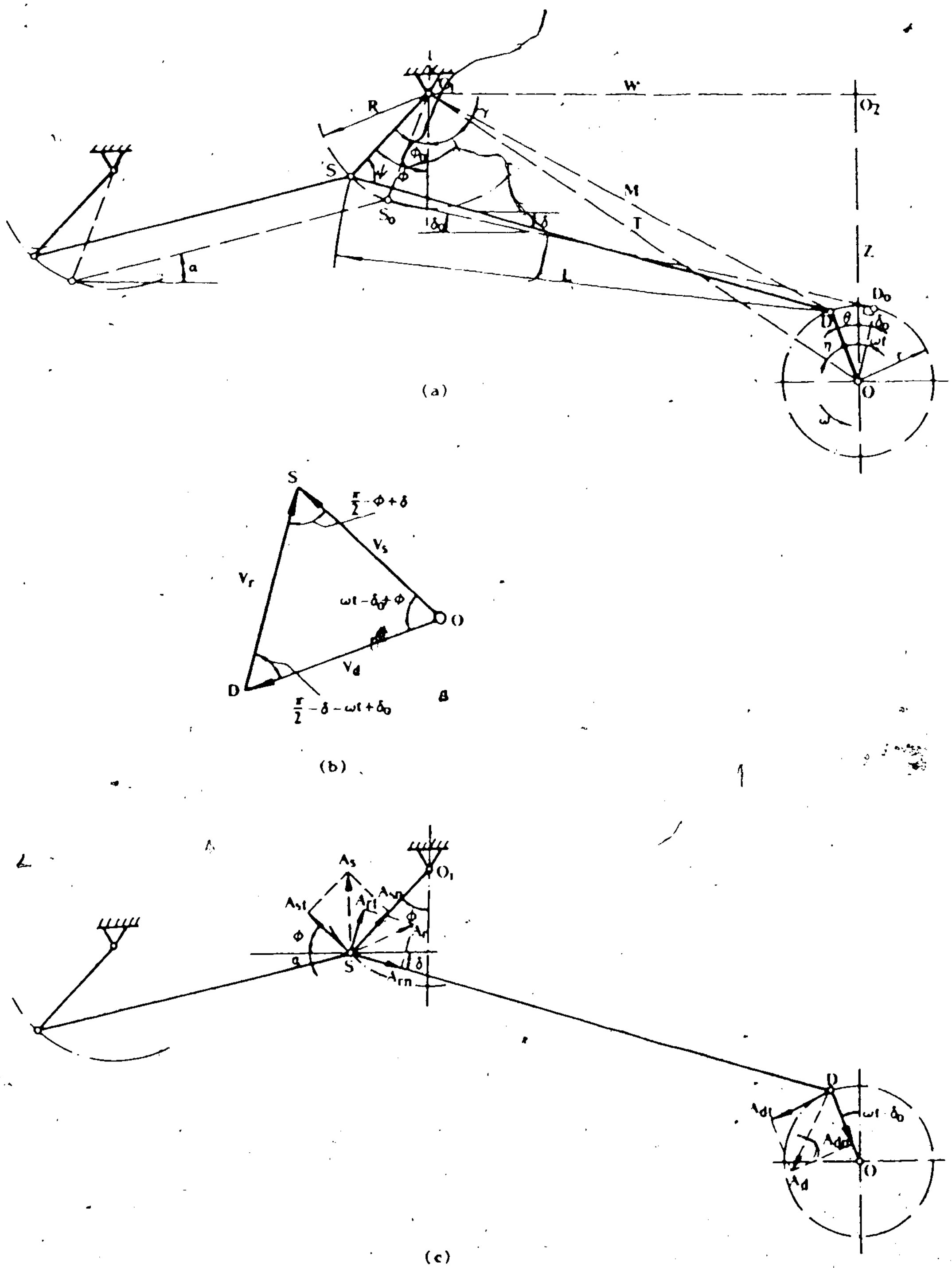

Fig. 3 An Oscillating Screen with the Crank-pitman Drive
(a) Geometric Relationships
(b) Velocity Polygon
(c) Acceleration Analysis

rotating counterclockwise in an angular velocity of ω. The hanger length is R and the pitman length is L. At any time t, the crank has turned an angle ωt, the new positions of the crank, pitman and hanger are shown by the solid lines (O_1SDO) in Fig. 3 a. The screen slope angle is α and hanger angle is ϕ. To find the geometric relationships, two auxiliary lines, O_1O and O_1D, are added which have the lengths of T and M respectively; then from Fig. 3 a,

$$W = L\cos\delta_o - R\sin\phi_o - r\sin\delta_o$$

$$Z = L\sin\delta_o + R\cos\phi_o + r\cos\delta_o$$

$$T = (W^2+Z^2)^{1/2}$$

$$\lambda = \tan^{-1}(W/Z)$$

In triangle O_1OD,

$$\eta = \lambda - \omega t + \delta_o$$

$$M = (T^2+r^2-2Tr\cos\eta)^{1/2}$$

By the rule of sines,

$$r/\sin\gamma = M/\sin\eta$$

or $\gamma = \sin^{-1}[(r/M)\sin\eta]$

In triangle O_1SD, by the rule of cosines,

$$L^2 = R^2+M^2-2RM\cos(\phi+\lambda+\gamma)$$

Then,

$$\phi = \cos^{-1}[(R^2+M^2-L^2)/(2RM)]-\lambda-\gamma \quad (1)$$

Also, $M^2 = L^2+R^2-2LR\cos\psi$

$$\psi = \cos^{-1}[(L^2+R^2-M^2)/(2LR)]$$

Since $\psi-\delta = (\pi/2)-\phi$

then, $\delta = \psi+\phi-(\pi/2)$ (2)

With the equations above, the hanger angle ϕ and the pitman slope angle δ at any time can be determined.

4.2.1.2 Velocity Analysis

As stated earlier, the motion state of the screen can be represented by that of one point such as point S in Fig. 3. According to the method of relative velocity (Barton 1984), the velocity of point S (V_s) is the vectorial summation of the velocity of point D (V_d) and the velocity of point S relative to point D (V_r); i.e.,

$$V_s = V_d + V_r \qquad (3)$$

Here, the capital V denotes the velocity vector and a small v will be used to denote the velocity magnitude.

The velocity polygon is shown by Fig. 3 b in which the angles between every two velocity vectors are also indicated; then, from the rule of sines,

$$v_s/\sin[(\pi/2)-\delta-\omega t+\delta_o] = v_r/\sin(\omega t-\delta_o+\phi)$$
$$= v_d/\sin[(\pi/2)-\phi+\delta]$$

or

$$v_s/\cos(\omega t+\delta-\delta_o) = v_r/\sin(\omega t-\delta_o+\phi)$$
$$= v_d/\cos(\phi-\delta)$$

Since $v_d = \omega r$

then

$$v_r = \omega r\sin(\omega t-\delta_o+\phi)/\cos(\phi-\delta) \qquad (4)$$

$$v_s = \omega r\cos(\omega t+\delta-\delta_o)/\cos(\phi-\delta) \qquad (5)$$

The screen velocity components parallel and perpendicular to the screen surface are respectively;

$$v_{sp} = v_s\cos(\phi+\alpha) \qquad (6)$$

$$v_{sv} = v_s\sin(\phi+\alpha) \qquad (7)$$

Here subscripts p and v denote parallel and perpendicular components respectively. Down-slope parallel velocity and upward perpendicular velocity are assumed positive.

4.2.1.3 Acceleration Analysis

To find the acceleration of point S (A_s) the method of relative acceleration (Barton 1984) is applied which states:

$$A_s = A_d + A_r \tag{8}$$

where A_d is the acceleration of point D and A_r is the acceleration of point S relative to point D. Here also the capital A is to denote the acceleration vector and a small a will be used to denote the acceleration magnitude.

Each of the three acceleration vectors in equation 8 can be resolved into two components; one is tangential and the other is normal to the direction of the corresponding velocity (the directions of the velocities are shown by the velocity polygon in Fig. 3 b). The resolution of the three acceleration vectors is illustrated in Fig. 3 c. Equation 8 can then be accordingly expanded into a normal and tangential component form:

$$A_{sn} + A_{st} = A_{dn} + A_{dt} + A_{rn} + A_{rt} \tag{9}$$

where subscripts n and t denote normal and tangential components respectively.

By noticing their directions shown in Fig. 3 c, the acceleration components in equation 9 can be expressed in exponential form as follows (Barton 1984);

$$A_{sn} = [(v_s)^2/R]e^{i[(\pi/2)-\phi]}$$

$$A_{st} = a_{st}e^{(\pi-\phi)}$$

$$A_{dn} = \omega^2 re^{-i[(\pi/2)-\omega t+\delta_0]}$$

$$A_{dt} = 0 \text{ (Constant crank angular velocity)}$$

$$A_{rn} = [(v_r)^2/L]e^{-i\delta}$$

$$A_{rt} = a_{rt}e^{i[(\pi/2)-\delta]}$$

where a_{st} denotes the magnitude of A_{st}, the tangential acceleration component of point S; and a_{rt} denotes the magnitude of A_{rt}, the tangential acceleration component of point S relative to point D.

Substitute the expressions above into equation 9,

$$[(v_s)^2/R]e^{i[(\pi/2)-\phi]}+a_{st}e^{i(\pi-\phi)}$$
$$= \omega^2 re^{-i[(\pi/2)-\omega t+\delta_0]}$$
$$+[(v_r)^2/L]e^{-i\delta}+a_{rt}e^{i[(\pi/2)-\delta]} \qquad (10)$$

Equating the real and the imaginary parts on both sides of equation 10 respectively yields

$$[(v_s)^2/R]\sin\phi-a_{st}\cos\phi = \omega^2 r\sin(\omega t-\delta_0)$$
$$+[(v_r)^2/L]\cos\delta+a_{rt}\sin\delta \qquad (11)$$

$$[(v_s)^2/R]\cos\phi+a_{st}\sin\phi = -\omega^2 r\cos(\omega t-\delta_0)$$
$$-[(v_r)^2/L]\sin\delta+a_{rt}\cos\delta \qquad (12)$$

In equations 11 and 12, a_{st} and a_{rt} are the only unknowns. By putting

$$A_1 = \cos\phi$$

$$A_2 = -\sin\phi$$

$$B_1 = \sin\delta$$

$$B_2 = \cos\delta$$

$$C_1 = [(v_s)^2/R]\sin\phi-\omega^2 r\sin(\omega t-\delta_0)-[(v_r)^2/L]\cos\delta$$

$$C_2 = [(v_s)^2/R]\cos\phi+\omega^2 r\cos(\omega t-\delta_0)+[(v_r)^2/L]\sin\delta$$

and solving equations 11 and 12 simultaneously, we get

$$a_{st} = (C_1B_2-C_2B_1)/(A_1B_2-A_2B_1) \tag{13}$$

$$a_{rt} = (C_2A_1-C_1A_2)/(A_1B_2-A_2B_1) \tag{14}$$

The total acceleration of the screen is,

$$a_s = [(a_{st})^2+(a_{sn})^2]^{1/2}$$
$$= [(a_{st})^2+(v_s)^4/R^2]^{1/2} \tag{15}$$

The acceleration components parallel and perpendicular to the screen surface are (see Fig. 3 c);

$$a_{sp} = a_{st}\cos(\phi+\alpha)+a_{sn}\cos[(\pi/2)+\phi+\alpha]$$
$$= a_{st}\cos(\phi+\alpha)-a_{sn}\sin(\phi+\alpha) \tag{16}$$

$$a_{sv} = a_{st}\sin(\phi+\alpha)+a_{sn}\sin[(\pi/2)+\phi+\alpha]$$
$$= a_{st}\sin(\phi+\alpha)+a_{sn}\cos(\phi+\alpha) \tag{17}$$

Here subscripts p and v are also used to denote parallel and perpendicular components of the screen acceleration respectively. The parallel component a_{sp} is positive when its direction is down the screen slope, and the perpendicular component a_{sv} is positive when its direction is upward.

4.2.2 Oscillating Screen with Bent-shaft Drive

4.2.2.1 Geometric Relationships

The schematic of an oscillating screen with a bent-shaft drive is shown in Fig. 4, in which drawing a shows the initial positions. Suppose that when time t is zero, the bent shaft OF is horizontal (Fig. 4 a), the swing bar DO is then vertical, and the connecting rod SD is also horizontal hence perpendicular to the swing bar. At any time t, the crank has rotated an angle ωt (see Fig. 4 b), the swing bar has turned an angle θ, the hanger angle is ϕ and the connecting rod has a slope angle δ with respect to the horizontal. O_1D and O_1O are connected with two auxiliary lines which have the lengths of M and T repectively.

From the initial positions shown in Fig. 4 a,

$$W = L - R\sin\phi_o$$

$$Z = r + R\cos\phi_o$$

and from Fig. 4 b,

$$T = (W^2+Z^2)^{1/2}$$

$$\lambda = \tan^{-1}(W/Z)$$

From the geometry of the bent-shaft,

$$\tan\theta = (r_1\sin\omega t)/P = \tan\beta\sin\omega t$$

or $$\theta = \tan^{-1}(\tan\beta\sin\omega t) \qquad (18)$$

In triangle O_1OD in Fig. 4 b,

$$\eta = \lambda - \theta$$

$$M = (T^2+r^2-2Tr\cos\eta)^{1/2}$$

$$M/\sin\eta = r/\sin\gamma$$

or $$\gamma = \sin^{-1}[(r/M)\sin\eta]$$

In triangle O_1SD, by cosine rule,

$$L^2 = R^2+M^2-2RM\cos(\phi+\lambda+\gamma)$$

$$\phi = \cos^{-1}[(R^2+M^2-L^2)/(2RM)]-\lambda-\gamma \qquad (19)$$

Also, $M^2 = R^2+L^2-2RL\cos\psi$

$$\psi = \cos^{-1}[(R^2+L^2-M^2)/(2RL)]$$

Since $\psi-\delta = (\pi/2)-\phi$

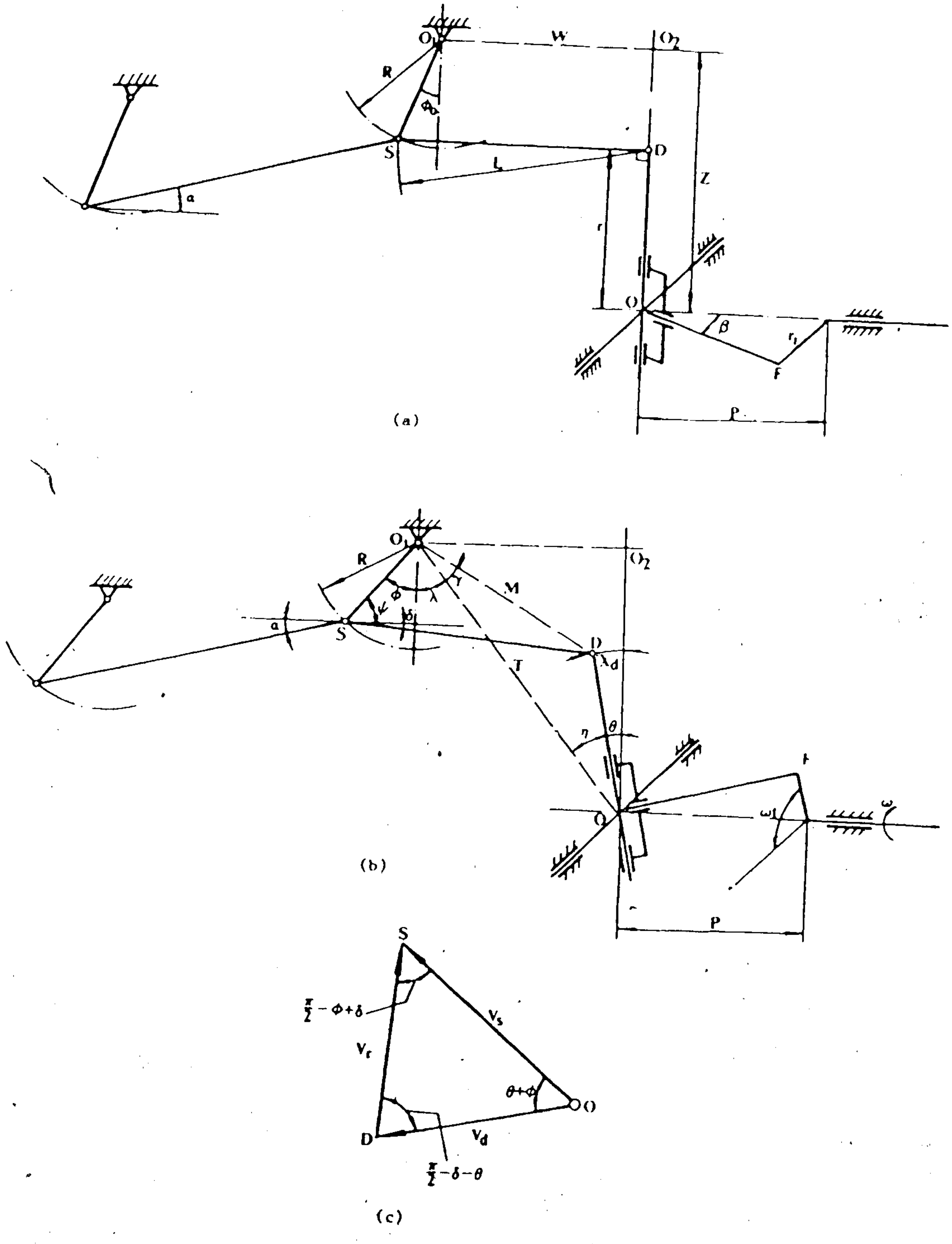

Fig. 4 An Oscillating Screen with the Bent-shaft Drive
(a) Initial Positions
(b) Geometric Relationships
(c) Velocity Polygon

$$\delta = \psi-(\pi/2)+\phi \qquad (20)$$

The hanger angle and the slope angle of the connecting rod at any time can be determined with equations 19 and 20.

4.2.2.2 Velocity Analysis

In the analysis hereinafter, the notations and sign conventions pertinent to velocities and accelerations defined in the previous section will be followed.

To determine the velocity of the screen, the output velocity of the drive, i.e. the velocity of point D, must be found first.

The linear displacement of point D is given by

$$X_d = r\theta$$

and with reference to equation 18,

$$X_d = r\tan^{-1}(\tan\beta\sin\omega t)$$

Differentiation of X_d with respect to time t yields the velocity of point D as given by Chen (1972):

$$v_d = (r\omega\tan\beta\cos\omega t)/(1+\tan^2\beta\sin^2\omega t) \qquad (21)$$

Applying the method of relative velocity (equation 3) on the connecting rod gives the velocity polygon shown in Fig. 4 c. From sine rule,

$$v_s/\sin[(\pi/2)-\delta-\theta] = v_r/\sin(\theta+\phi) = v_d/\sin[(\pi/2)-\phi+\delta]$$

or $\quad v_s/\cos(\delta+\theta) = v_r/\sin(\theta+\phi) = v_d/\cos(\phi-\delta)$

then,

$$v_r = v_d\sin(\theta+\phi)/\cos(\phi-\delta) \qquad (22)$$

$$v_s = v_d\cos(\delta+\theta)/\cos(\phi-\delta) \qquad (23)$$

The velocity components parallel and perpendicular to the screen surface are still given by equation 6 and 7 respectively;

$$v_{sp} = v_s\cos(\phi+\alpha)$$

$$v_{sv} = v_s\sin(\phi+\alpha)$$

4.2.2.3 **Acceleration Analysis**

To determine the acceleration of the screen, the method of relative acceleration is applied which gives equation 9:

$$A_{sn}+A_{st} = A_{dn}+A_{dt}+A_{rn}+A_{rt} \qquad (9)$$

Here, (see Fig. 4 b)

$$A_{sn} = [(v_s)^2/R]e^{i[(\pi/2)-\phi]}$$

$$A_{st} = a_{st}e^{i(\pi-\phi)}$$

$$A_{dn} = [(v_d)^2/r]e^{-i[(\pi/2)-\theta]}$$

$$A_{dt} = a_{dt}e^{i(\pi+\theta)}$$

$$A_{rn} = [(v_r)^2/L]e^{-i\delta}$$

$$A_{rt} = a_{rt}e^{i[(\pi/2)-\delta]}$$

Substituting the expressions above into equation 9, we get

$$[(v_s)^2/R]e^{i[(\pi/2)-\phi]}+a_{st}e^{i(\pi-\phi)}$$
$$= [(v_d)^2/r]e^{-i[(\pi/2)-\theta]}+a_{dt}e^{i(\pi+\theta)}$$
$$+[(v_r)^2/L]e^{-i\delta}+a_{rt}e^{i[(\pi/2)-\delta]} \qquad (24)$$

Equating the real and the imaginary parts on both sides of equation 24 respectively gives

$$[(v_s)^2/R]\sin\phi-a_{st}\cos\phi = [(v_d)^2/r]\sin\theta-a_{dt}\cos\theta$$
$$+[(v_r)^2/L]\cos\delta+a_{rt}\sin\delta \qquad (25)$$

and

$$(v_s)^2/R\cos\phi+a_{st}\sin\phi = -[(v_d)^2/r]\cos\theta-a_{dt}\sin\theta$$
$$-[(v_r)^2/L]\sin\delta+a_{rt}\cos\delta \qquad (26)$$

In equations 25 and 26, a_{dt} can be determined by differentiating v_d (equation 21) with respect to time t.

$$a_{dt} = dv_d/dt = \{-\omega^2 r\tan\beta\sin\omega t[1+\tan^2\beta(1+\cos^2\omega t)]\}/[1+\tan^2\beta\sin^2\omega t]^2 \qquad (27)$$

Then a_{st} and a_{rt} are the only two unknowns left in equations 25 and 26. By putting

$$A_1 = \cos\phi$$

$$A_2 = -\sin\phi$$

$$B_1 = \sin\delta$$

$$B_2 = \cos\delta$$

$$C_1 = [(v_s)^2/R]\sin\phi-[(v_d)^2/r]\sin\theta + a_{dt}\cos\theta-[(v_r)^2/L]\cos\delta$$

$$C_2 = [(v_s)^2/R]\cos\phi+[(v_d)^2/r]\cos\theta + a_{dt}\sin\theta+[(v_r)^2/L]\sin\delta$$

and solving the two equations simultaneously, we get equations 13 and 14;

$$a_{st} = (C_1B_2-C_2B_1)/(A_1B_2-A_2B_1)$$

$$a_{rt} = (C_2A_1-C_1A_2)/(A_1B_2-A_2B_1)$$

Then, the total acceleration of the screen is given by equation 15,

$$a_s = [(a_{st})^2+(a_{sn})^2]^{1/2} = [(a_{st})^2+(v_s)^4/R^2]^{1/2}$$

and the acceleration components parallel and perpendicular to the screen surface are given by equations 16 and 17 respectively

$$a_{sp} = a_{st}\cos(\phi+\alpha)-a_{sn}\sin(\phi+\alpha)$$

$$a_{sv} = a_{st}\sin(\phi+\alpha)+a_{sn}\cos(\phi+\alpha)$$

4.2.3 Oscillating Screen with Spatial Crank Drive

4.2.3.1 Geometric Relationships

The spatial crank-slider connected to a screen is shown by the schematic in Fig. 5 in which FO is the spatial crank. The initial positions are shown by drawing a. Suppose that when time t is zero, the crank is horizontal, the connecting rod SD is in alignment with the slider DE hence is also horizontal, point D is at D_o and the hanger angle is ϕ_o. At any time t, the crank has turned an angle ωt, point D has moved a distance X_d from D_o, the hanger angle and the connecting rod slope angle are respectively ϕ and δ as shown by Fig. 5 b. To find the geometric relationships O_1D_o and O_1D are connected with two auxiliary lines that have the lengths of T and M respectively.

From the initial positions shown in Fig. 5 a,

$$W = L - R\sin\phi_o$$

$$Z = R\cos\phi_o$$

and from Fig. 5 b,

$$T = (W^2+Z^2)^{1/2}$$

$$\lambda = \tan^{-1}(W/Z)$$

At any time t the horizontal displacement of joint F can be found from the geometry of the drive (Fig. 5 b) as follows:

$$f = r\sin\omega t\cos(\pi/2-\beta) = r\sin\beta\sin\omega t$$

Then the displacement of point D given by Chen (1972) is

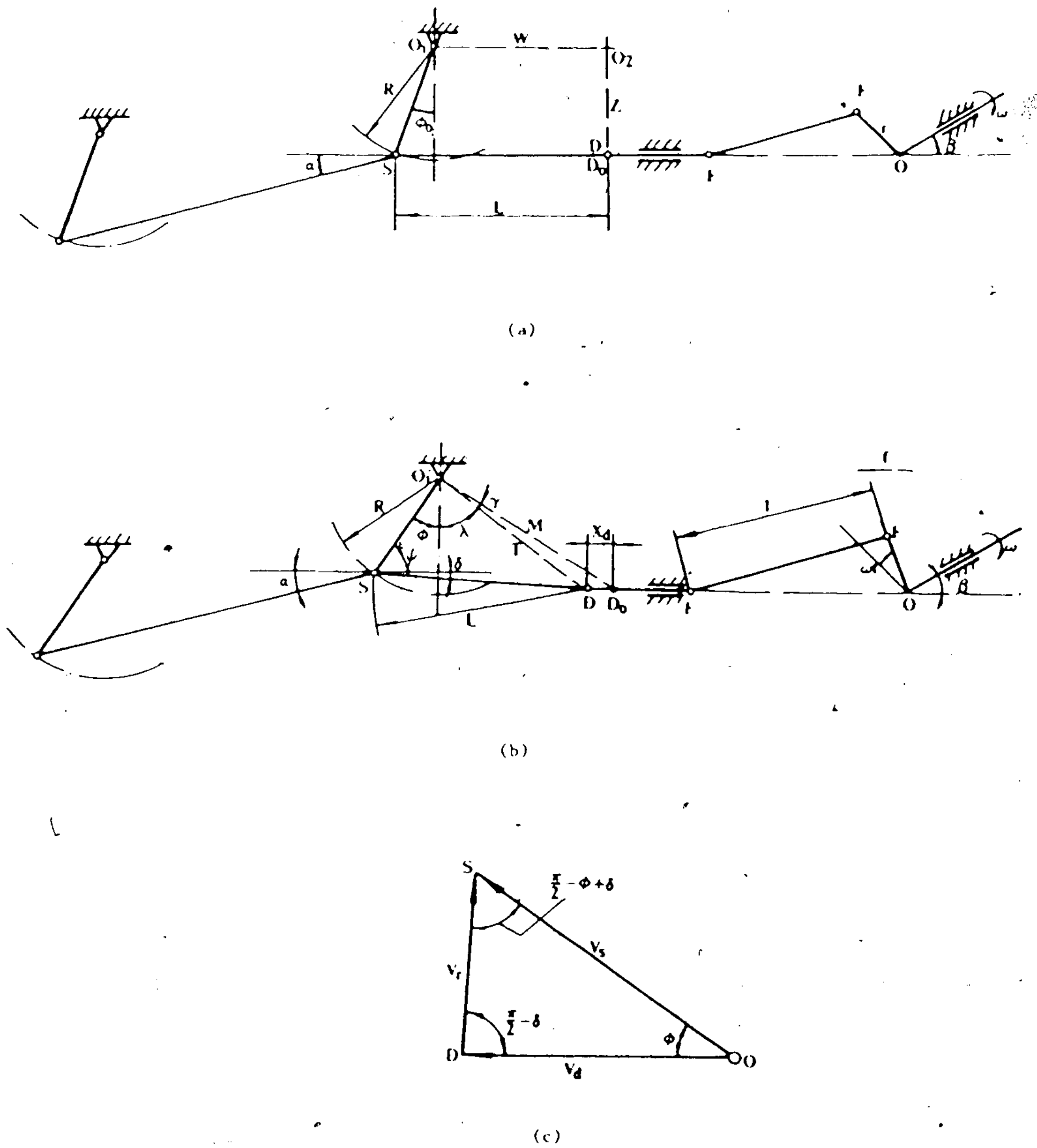

Fig.5 An Oscillating Screen with the Spatial Crank Drive
(a) Initial Positions
(b) Geometric Relationships
(c) Velocity Polygon

$$X_d = (l^2-r^2+f^2)^{1/2}+f-(l^2-r^2)^{1/2}$$

Putting $u = (l^2-r^2+f^2)^{1/2}$, then

$$X_d = u+f-(l^2-r^2)^{1/2} \quad (28)$$

In triangle O_1DD_o in Fig. 5 b,

$$M = (T^2+X_d{}^2-2TX_d\sin\lambda)^{1/2}$$

$$M/\sin(\pi/2-\lambda) = X_d/\sin\gamma$$

$$\gamma = \sin^{-1}[(X_d/M)\cos\lambda]$$

In triangle O_1SD (Fig. 5 b),

$$L^2 = R^2+M^2-2RM\cos(\phi+\lambda-\gamma)$$

thus,

$$\phi = \cos^{-1}[(R^2+M^2-L^2)/(2RM)]-\lambda+\gamma \quad (29)$$

and $M^2 = R^2+L^2-2RL\cos\psi$

$$\psi = \cos^{-1}[(R^2+L^2-M^2)/(2RL)]$$

$$\delta = \psi-(\pi/2)+\phi \quad (30)$$

4.2.3.2 Velocity Analysis

The output velocity of the drive, v_d, can be found by differentiating X_d (equation 28) with respect to time t.

$$v_d = dX_d/dt = [(f/u)+1]k\omega \quad (31)$$

where $k = r\sin\beta\cos\omega t$

The application of the method of relative velocity on the connecting rod gives the velocity polygon shown by Fig. 5 c.

From sine rule,

$$v_s/\sin[(\pi/2)-\delta] = v_r/\sin\phi = v_d/\sin[(\pi/2)-\phi+\delta]$$

Then

$$v_r = v_d\sin\phi/\cos(\phi-\delta) \quad (32)$$

$$v_s = v_d\cos\delta/\cos(\phi-\delta) \tag{33}$$

The velocity components parallel and perpendicular to the screen surface are again given by equations 6 and 7 respectively;

$$v_{sp} = v_s\cos(\phi+\alpha)$$

$$v_{sv} = v_s\sin(\phi+\alpha)$$

4.2.3.3 Acceleration Analysis

Equation 9, written according to the method of relative acceleration, is again applied.

$$A_{sn}+A_{st} = A_{dn}+A_{dt}+A_{rn}+A_{rt} \tag{9}$$

Here, from Fig. 5 b,

$$A_{sn} = [(v_s)^2/R]e^{i[(\pi/2)-\phi]}$$

$$A_{st} = a_{st}e^{i(\pi-\phi)}$$

$$A_{dn} = 0 \text{ (Since } V_d \text{ is always horizontal)}$$

$$A_{dt} = a_{dt}e^{i\pi}$$

$$A_{rn} = [(v_r)^2/L]e^{-i\delta}$$

$$A_{rt} = a_{rt}e^{i[(\pi/2)-\delta]}$$

Substituting the expressions above into equation 9, we get

$$[(v_s)^2/R]e^{i[(\pi/2)-\phi]}+a_{st}e^{i(\pi-\phi)} = a_{dt}e^{i\pi} +[(v_r)^2/L]e^{-i\delta}+a_{rt}e^{i[(\pi/2)-\delta]} \tag{34}$$

Equating the real and the imaginary parts on both sides of equation 34 gives;

$$[(v_s)^2/R]\sin\phi-a_{st}\cos\phi = -a_{dt}+[(v_r)^2/L]\cos\delta+a_{rt}\sin\delta \tag{35}$$

and,

$$[(v_s)^2/R]\cos\phi+a_{st}\sin\phi$$
$$= -[(v_r)^2/L]\sin\delta+a_{rt}\cos\delta \qquad (36)$$

a_{dt} can be obtained by differentiating v_d (equation 31) with respect to time t.

$$a_{dt} = dv_d/dt = -[f(f/u+1)-k^2/u(f^2/u^2-1)]\omega^2 \qquad (37)$$

Now, in equations 35 and 36, only a_{st} and a_{rt} are left unknown. By putting

$$A_1 = \cos\phi$$
$$A_2 = -\sin\phi$$
$$B_1 = \sin\delta$$
$$B_2 = \cos\delta$$
$$C_1 = [(v_s)^2/R]\sin\phi+a_{dt}-[(v_r)^2/L]\cos\delta$$
$$C_2 = [(v_s)^2/R]\cos\phi+[(v_r)^2/L]\sin\delta$$

and solving the equations simultaneously, we again get equations 13 and 14;

$$a_{st} = (C_1B_2-C_2B_1)/(A_1B_2-A_2B_1)$$
$$a_{rt} = (C_2A_1-C_1A_2)/(A_1B_2-A_2B_1)$$

Then the total acceleration of the screen is also given by equation 15,

$$a_s = [(a_{st})^2+(a_{sn})^2]^{1/2}$$
$$= [(a_{st})^2+(v_s)^4/R^2]^{1/2}$$

and the acceleration components parallel and perpendicular to the screen surface are given by equations 16 and 17 respectively;

$$a_{sp} = a_{st}\cos(\phi+\alpha)-a_{sn}\sin(\phi+\alpha)$$
$$a_{sv} = a_{st}\sin(\phi+\alpha)+a_{sn}\cos(\phi+\alpha)$$

4.2.4 Oscillating Screen with Quick-return Drive

4.2.4.1 Geometric Relationships

The schematic of an oscillating screen with a quick-return drive is shown in Fig. 6 in which OB is the crank length r, OO_3 is the center distance h, and DO_3 is the swing-bar height H. H/h is called the swing-bar height/center distance ratio (e) or the bar/center ratio for short. Fig. 6 a shows the initial positions. Suppose that when time t is zero, the swing bar is vertical and is in alignment with the crank, and the connecting rod SD is horizontal. B is a point on the slider and B' is the coincident point of point B on the swing-bar. Because of the structural resemblance, the oscillating screen with a quick-return drive has the same geometric relationships as the one with a bent-shaft drive. To use those equations developed in 4.2.2.1, the same notations as those in Fig. 4 are used for the equivalent dimensions and angles in Fig. 6 except that the swing-bar height is noted as H instead of r. Also the value of θ is no longer given by equation 18. Rather, from triangle OBO_3 in Fig. 6 b and cosine rule,

$$l = [r^2+h^2-2rh\cos(\pi-\omega t)]^{1/2}$$

$$= (r^2+h^2+2rh\cos\omega t)^{1/2}$$

and from sine rule,

$$r/\sin\theta = l/\sin(\pi-\omega t)$$

then, $$\theta = \sin^{-1}[(r/l)\sin\omega t] \qquad (38)$$

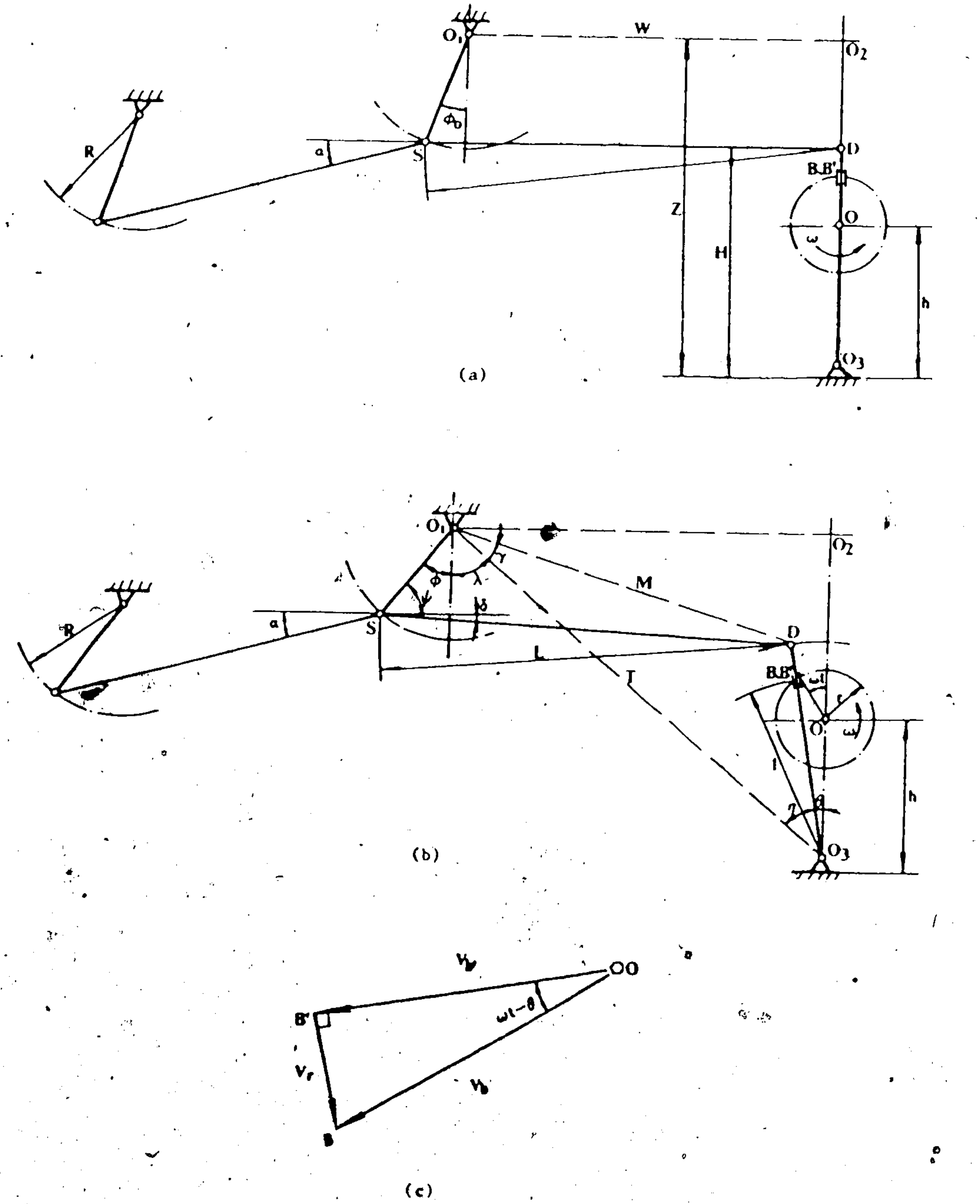

Fig. 6 An Oscillating Screen with the Quick-return Drive
(a) Initial Positions
(b) Geometrical Relationships
(c) Velocity Polygon for The Drive

4.2.4.2 Velocity Analysis

The output velocity of the drive must be determined first in order to obtain the screen velocity. At any time t, the linkage positions and the velocity polygon for the drive are shown by Fig. 6 b and c respectively. In the velocity polygon, V_b and $V_{b'}$ are the velocities of point B and point B' respectively, and V_r is the velocity of point B relative to point B'.

Since $v_b = \omega r$

then from the velocity polygon,

$$v_{b'} = v_b \cos(\omega t - \theta) = \omega r \cos(\omega t - \theta) \qquad (39)$$

$$v_r = v_b \sin(\omega t - \theta) = \omega r \sin(\omega t - \theta) \qquad (40)$$

Therefore, the velocity of point D, i.e. the output velocity of the drive,

$$v_d = (H/l) v_{b'}$$

$$= (H/l)\omega r \cos(\omega t - \theta) \qquad (41)$$

With the velocity of point D (v_d) given by equation 41, the velocities of the screen can be determined with the equations developed previously (4.2.2.2) because of the structural similarity between the oscillating screen with the quick-return drive and the one with the bent-shaft drive. The velocity of the screen (v_s) is given by equation 23 and the velocity of point S relative to point D (v_r) is given by equation 22. Equations 24 and 25 give the velocity components parallel and perpendicular to the screen surface respectively.

4.2.4.3 Acceleration Analysis

In the acceleration analysis, the acceleration of point B' and consequently that of point D must be determined first by using the method of relative accelration which gives

$$A_b = A_{b'} + A_r$$

or $$A_{bn} + A_{bt} = A_{b'n} + A_{b't} + A_{rn} + A_{rt} + A_{rc} \qquad (42)$$

where A_b is the acceleration of point B,

$A_{b'}$ is the acceleration of point B',

A_r is the acceleration of point B relative to point B',

A_{rc} is the Coriolis acceleration of point B relative to point B',

and the second subscripts t and n still denote the acceleration components tangential and the normal to the directions of the corresponding velocities respectively.

By examining the motion and the geometry of the drive from Fig. 6 b, we get

$$A_{bn} = -\omega^2 r e^{i[(\pi/2)+\omega t]}$$

$$A_{bt} = 0 \text{ (Constant crank angular velocity)}$$

$$A_{b'n} = -[(v_{b'})^2/l]e^{i[(\pi/2)+\theta]}$$

$$A_{b't} = a_{b't}e^{i(\pi+\theta)}$$

$$A_{rn} = 0 \text{ (Linear relative motion)}$$

$$A_{rt} = -a_{rt}e^{i[(\pi/2)+\theta]}$$

$$A_{rc} = 2v_r(v_{b'}/l)e^{i\theta}$$

Substituting the expressions above into equation 42 and equating the real and imaginary parts respectively yield;

$$\omega^2 r\sin(\omega t) = [(v_{b'})^2/l]\sin\theta - a_{b't}\cos\theta + a_{rt}\sin\theta + 2v_r(v_{b'}/l)\cos\theta \quad (43)$$

$$-\omega^2 r\cos(\omega t) = -[(v_{b'})^2/l]\cos\theta - a_{b't}\sin\theta - a_{rt}\cos\theta + 2v_r(v_{b'}/l)\sin\theta \quad (44)$$

Putting

$$a_1 = \cos\theta$$

$$a_2 = \sin\theta$$

$$b_1 = -\sin\theta$$

$$b_2 = \cos\theta$$

$$c_1 = [(v_{b'})^2/l]\sin\theta + 2v_r(v_{b'}/l)\cos\theta - \omega^2 r\sin(\omega t)$$

$$c_2 = -[(v_{b'})^2/l]\cos\theta + 2v_r(v_{b'}/l)\sin\theta + \omega^2 r\cos(\omega t)$$

and solving equations 43 and 44 simultaneously give;

$$a_{b't} = (c_1b_2 - c_2b_1)/(a_1b_2 - a_2b_1) \quad (45)$$

$$a_{rt} = (c_2a_1 - c_1a_2)/(a_1b_2 - a_2a_1) \quad (46)$$

Owing to the proportionality of acceleration, the tangential acceleration of point D is given by

$$a_{dt} = (H/l)a_{b't} \quad (47)$$

The normal acceleration of point D can be determined with the velocity of point D (v_d), which is given by equation 41, and the hanger length (R). The accelerations of the screen can be determined with the equations developed in 4.2.2.3 again because of the similarity between the oscillating screen with the bent-shaft drive and the one with the quick-return drive. The tangential acceleration of the screen can be found by using equation 13 and the normal acceleration can be determined with the velocity of the screen and the hanger length. The acceleration components parallel and perpendicular to the screen surface are given by equations 16 and 17.

4.3 Motion of the Particle

The movement of the screen causes the particles to move which are in contact with it. According to the assumptions made in 4.1, the particle may not roll on the screen, but as Schertz and Hazen (1963) noticed, it may hop, ride, slide, or ride and slide on the screen surface.

The mode of particle motion is important to the screening effectiveness. There is no opportunity for the particle to pass through a perforation if it loses contact with the screen such as in the hopping mode, and when the particle is riding on the screen, it cannot find a perforation to pass through. For effective screening, hopping and riding are, therefore, not the desirable modes of particle motion. Garvie (1966) stated that, to obtain maximum effectiveness of separation, continuous sliding up and down of the particles on the screen is the most favorable type of motion; consequently, in this study, the values for the variables will be determined in such a way that they keep the particle in a *continuous sliding* motion only.

When a particle with a mass of m is sliding on an oscillating screen with a slope angle of α, its free-body diagram is shown in Fig. 7. The acceleration component of

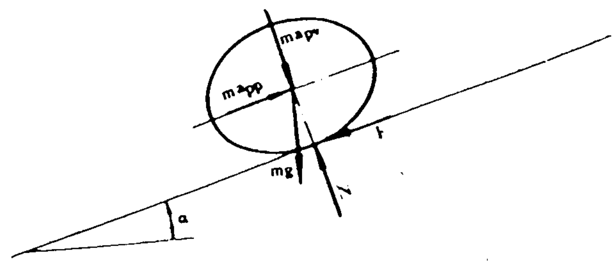

Fig. 7 The Free-body Diagram of a Particle Situating on an Inclined Oscillating Surface

the particle parallel to the screen surface, A_{pp}, is assumed to be positive when its direction is down the screen slope, and the component perpendicular to the screen surface, A_{pv}, is positive when its direction is upward; then, the positive directions of the inertia forces associated with the two acceleration components, ma_{pp} and ma_{pv} respectively, are as shown in the diagram. The frictional force F acted on the particle is also drawn in the assumed positive direction. N is the normal contact force and mg is the force of gravity or weight of the particle.

Consideration of the equilibrium of the particle gives

$$ma_{pp} = F+mg\sin\alpha \tag{48}$$

$$ma_{pv} = N-mg\cos\alpha \tag{49}$$

Since continuous sliding also means constant contact of the particle with the screen surface, then in the direction perpendicular to the screen surface, the acceleration of the particle is the same as that of the screen; that is,

$$a_{pv} = a_{sv}$$

Then from equation 49,

$$N = ma_{pv}+mg\cos\alpha = ma_{sv}+mg\cos\alpha$$

Though continuous sliding is assumed, at the instant when the particle changes its direction of motion with respect to the screen, the relative particle to screen velocity is zero. If sliding is renewed instantaneously, however, it is not necessary to consider static friction since friction does not return immediately to its static value when the sliding object returns to rest (Sampson et al. 1943, Feller and Foux 1975); therefore, the kinetic friction coefficient, μ_k, is considered to be in effect all the time. Then,

$$F = \mu_k N = \mu_k(ma_{sv}+mg\cos\alpha) \quad (50)$$

With the assumed positive direction shown in the diagram, F has the same sign as (v_s-v_p) where v_s is the velocity of the screen and v_p is the velocity of the particle. Then the sign of F can be determined by

$$\text{sign}(v_s-v_p)^*$$

Substitution of equation 50 into 48 with the sign of F included gives

$$ma_{pp} = \text{sign}(v_s-v_p)\mu_k(ma_{sv}+mg\cos\alpha)+mg\sin\alpha$$

then, $a_{pp} = \text{sign}(v_s-v_p)\mu_k(a_{sv}+g\cos\alpha)+g\sin\alpha \quad (51)$

* The sign function is defined as follows:
sign(x)=1 when x≥0, and sign(x)=-1 when x<0.

Equation 51 is the mathematical model of particle motion as the particle is confined to continuous sliding. It gives the acceleration of the particle and the integration of it yields the velocity. It can be noticed that the mass of the particle does not appear in equation 51 indicating that the motion of the particle is not affected by the mass.

4.4 Limit Velocities, Penetrating Ratio, Average Relative Velocity and Efficiency Index

When an undersized particle crosses a perforation it can fall; however, to fall through the perforation it is necessary for the particle to have a sufficiently low velocity with respect to the screen so that its mass center can fall below the screen surface before it meets the edge of the screen perforation, otherwise it will rebound up onto the screen surface again. In other words, there is a limit to the relative velocity at or below which the particle has enough time to fall through the perforation. Garvie (1966) listed an equation to determine the limit velocity (see section 2.5.3) but it was for a particle only moving down a sloping screen. Furthermore, it is not clear how the equation was derived; consequently, equations for determining the limit velocity were developed as follows for the particle moving both up and down a sloping screen.

Fig. 8 shows the moment when the mass center of a prolate particle is at the edge of a screen perforation with a down-slope relative velocity v_r. The length of the particle is 2b and the height is 2a; the screen has a slope angle of α and a perforation length of L. To pass through the perforation, the particle should fall into the

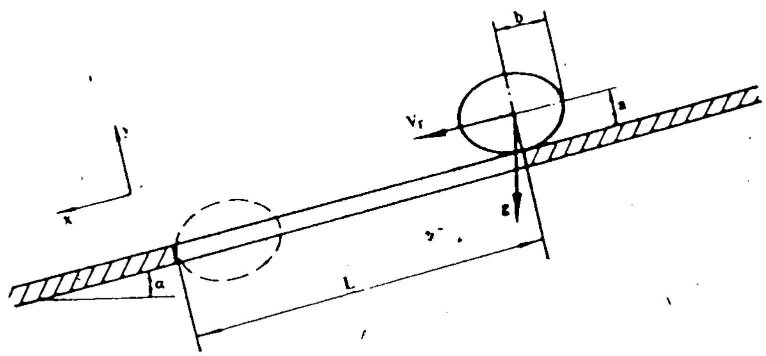

Fig. 8 A Particle Accessing a Perforation with a Down-slope Relative Velocity

perforation (in the -y direction) to at least one half of its height, a, when or before it travels a distance of (L-b) with respect to the screen in the x direction. i.e.,

$$v_r t+(1/2)t^2 g\sin\alpha \le L-b \qquad (52)$$

$$(1/2)t^2 g\cos\alpha = a \qquad (53)$$

where, g is the acceleration due to gravity,

t is the time.

From equation 53,

$$t = [2a/(g\cos\alpha)]^{1/2} \qquad (54)$$

Substitute equation 54 into equation 52 and rewrite,

$$v_r \le [2a/(g\cos\alpha)]^{1/2}\{[(L-b)/(2a)]g\cos\alpha-(1/2)g\sin\alpha\}$$

Then the limit velocity for the particle moving down the screen slope is

$$v_{ld} = [2a/(g\cos\alpha)]^{1/2}\{[(L-b)/(2a)]g\cos\alpha-(1/2)g\sin\alpha\} \qquad (55)$$

Garvie's equation (section 2.6.3) differs from equation 55, but the reasons for this difference are not known as his derivation is not presented. The two equations were compared by assigning some arbitrary values to the dimensions and the angle of screen slope. The results from the two equations were considerably different, and the difference increased with the screen slope angle and the particle dimensions. For horizontal screens, however, the two equations were identical.

Fig. 9 shows the particle accessing the perforation with an up-slope relative velocity. By following the same procedures as those for the down-slope limit velocity, the limit velocity for the up-slope moving particle, v_{lu}, can

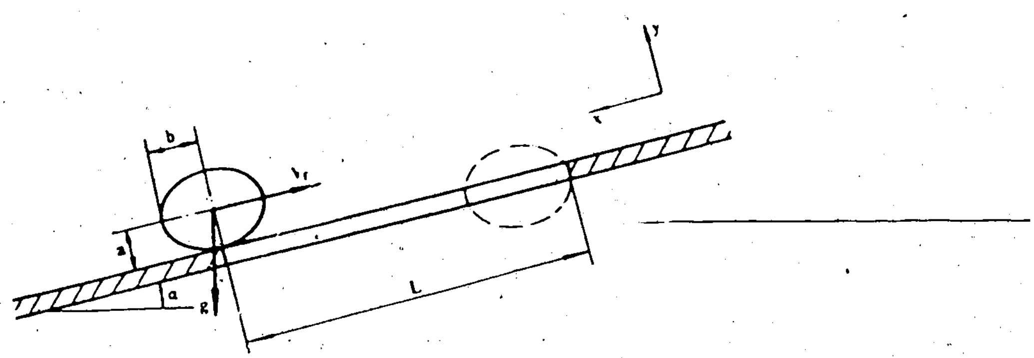

Fig. 9 A Particle Accessing a Perforation with an Up-slope Relative Velocity

also be easily found as

$$v_{1u} = [2a/(g\cos\alpha)]^{1/2}\{[(L-b)/(2a)]g\cos\alpha+(1/2)g\sin\alpha\} \quad (56)$$

Combining equations 55 and 56 together gives the general formula for the limit velocity, v_1,

$$v_1 = [2a/(g\cos\alpha)]^{1/2}\{[(L-b)/(2a)]g\cos\alpha\pm(1/2)g\sin\alpha\} \quad (57)$$

where, the plus sign is for the particle moving up the slope, and the minus sign is for the particle moving down the slope. As can be noted, the limit velocity is determined by the particle dimensions, the screen perforation length, the screen slope angle and the direction of particle motion relative to the screen; therefore, for a specific particle and a specific screen, the limit velocity is one of the two constant values depending on the direction of particle motion relative to the screen.

The particle velocity relative to the screen changes continuously. In one crank cycle or one period of oscillation, the relative velocity can be sometimes lower than the limit velocity and other times higher than the limit velocity. The particle can fall through a screen perforation only when the relative velocity is lower than the limit velocity (Harrison and Blecha 1983). In order to specify the opportunity of penetration, the fraction of the time when the relative velocity is lower than the limit velocity over one period of oscillation is defined as the penetrating ratio (ϵ).

Fig. 10 illustrates the screen and the particle velocities with the relative velocity being the difference

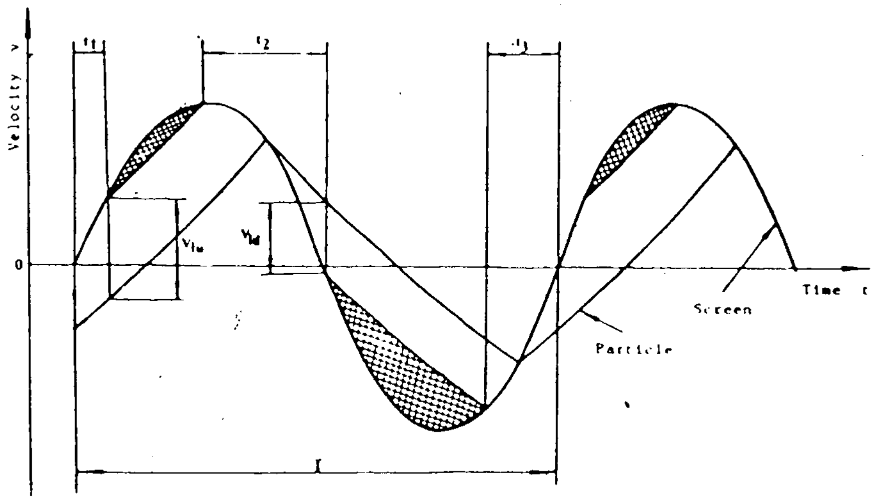

Fig. 10 Definition of the Penetrating Ratio

between the two. The up-slope limit velocity (v_{1u}) and the down-slope limit velocity (v_{1d}) are added to or subtracted from the particle velocity depending on the direction of the relative motion. The hatched areas show when and by how much the relative velocity is greater than the corresponding limit velocity, and t_1, t_2 and t_3 are the times when the particle velocity relative to the screen is lower than the limit velocities for one period of oscillation, T. According to the definition, the penetrating ratio is then given by

$$\epsilon = (t_1+t_2+t_3)/T \tag{58}$$

It can be seen that the maximum value for the penetrating ratio is one.

When a particle encounters a screen perforation, the chance that the relative velocity is lower than the limit velocity, and that the particle can pass through the perforation, is given by the penetrating ratio. The greater the penetrating ratio, the better the chance that the particle can penetrate the screen perforation. For example, if the penetrating ratio is 0.6, then for 60% of the time the relative velocity is lower than the limit velocity and there is a 60% chance that the particle can pass through a screen perforation when it encounters one perforation and is aligned with it. For a specific screen, the penetrating ratio also indicates the number of the perforations a particle fails to fall through before it penetrates the screen.

The average of the absolute value of the particle velocity relative to the screen is termed as the average relative velocity (v_{ar}); that is,

$$v_{ar} = \int |v_p - v_s| dt / \int dt \quad (59)$$

where, v_p is the particle velocity,

v_s is the screen velocity, and

t is the time.

The average relative velocity indicates the relative motion between the particle and the screen without regard to the direction of the motion. For a specific screen, the average relative velocity indicates the average number of perforations the particle can encounter in a given time period.

The time that a particle requires before it falls through a screen perforation is a function of two major factors; one is the number of perforations it can encounter in a given time period, the other is the number of the perforations it fails to penetrate. As noted above, the first factor is indicated by the average relative velocity, whereas the second factor is indicated by the penetrating ratio; therefore, the product of the average relative velocity and the penetrating ratio can imply the screening effectiveness or Efficiency Index (EI); that is,

$$EI = \epsilon v_{ar} \tag{60}$$

The higher the efficiency index is, the sooner a particle can penetrate a screen.

The average relative velocity and the penetrating ratio are not mutually exclusive. When one increases the other one may decrease, and a high average relative velocity or a high penetrating ratio may not necessarily produce a high efficiency index.

The average relative velocity, the penetrating ratio and the efficiency index are the dependent variables of the study. Their responses to the independent variables and drives noted in Chapter 3 are examined with the aid of a computational simulation model.

4.5 Computational Model

The equations developed previously for the screen and particle motions were put together to form the computational simulation model. The program was written in BASIC (See Appendix A.) and run on an IBM personal computer.

The model was developed to cope with the oscillating screen actuated by any of the four drives noted previously. All the variables listed in Chapter 3 were taken as the parameters of the model and the required values for them were entered from the keyboard after a particular drive was chosen.

The program was written on a time increment base. The time increment was 1/40 of the period of screen oscillation. For every time increment, the program can use, according to the choice of the driving mechanism, an appropriate set of equations to predict the state of screen motion; i.e. to calculate the accelerations and the velocities of the screen. The acceleration of the particle is then computed by using equation 51, and the velocity of the particle is determined from the acceleration by using the Runge-Kutta's Fourth Order Numerical Integration Rule (Speckhart and Green 1976).

The program checks the mode of particle motion regularly to guarantee that the particle is in continuous sliding motion only. If the relative particle to screen velocity is lower than 0.1 mm/s consecutively for two time increments, the particle is considered riding on the screen and the program execution stops. When the downward vertical acceleration of the screen is greater than 9.81 m/s^2 in magnitude and the particle loses contact with the screen, the program execution also stops.

The particle initially had no velocity or acceleration.

It was released onto the screen at the mid-stroke of oscillation. The velocity increases or decreases with the movement of the screen, but eventually the average particle velocity reaches a steady value and the motion of the particle enters a steady-pattern state. The program has a subroutine to monitor the motion of the particle. The subroutine calculates the average particle velocity for every cycle and compare the average velocities for every two consecutive cycles. If the difference of the average particle velocity between two consecutive cycles is less than 5 mm/s, the steady-pattern state of particle motion is considered reached. The program then starts the computation of the average relative velocity, the penetrating ratio and eventually the efficiency index.

The average relative velocity and the penetrating ratio for each cycle are first determined and stored in two separate arrays. The penetrating ratio is determined by finding the time when the relative velocity is lower than the limit velocity in one cycle. At the end of the program execution, the overall averages of the average relative velocity and of the penetrating ratio, and consequently the efficiency index are computed and printed out as the output results.

5. PROGRAM EXECUTION

5.1 Constants and Variables of the Model

The particle moving on the screen was assumed to be 6 mm long, 2.8 mm wide and 2.6 mm high. The dimensions are the mean values for wheat grains as measured by Edison and Brogan (1972). The orientation of the particle with respect to the direction of oscillation is a function of the natural rocking frequency (Hann and Gentry 1972). The natural rocking frequencies of grains such as wheat, barley and oats are all above 15 Hz (Harrison and Blecha 1983) which is higher than the frequency levels used for screen oscillation in this study; therefore, the particles would take an orientation with their long axes (or length) perpendicular to the plane of oscillation. The necessary dimensions of the particle, i.e. a and b in Fig. 8 and 9, were consequently 1.8 mm (2.6/2) and 1.9 mm (2.8/2) respectively. The perforation length (L in Fig. 8 and 9) was assigned the value of 4.5 mm.

The perforation length and the particle dimensions affect the limit velocities (equation 57), and consequently the penetrating ratio. Though such changes increase or decrease the penetrating ratio, the response pattern of the penetrating ratio is unchanged. The range of the penetrating ratio is from zero to one; therefore, the penetrating ratio will be one or zero if the chosen perforation length is too large or too small. The perforation length of 4.5 mm was chosen because a penetrating ratio of one was obtained for the lowest levels of the frequency and the amplitude, and yet was greater than zero for the highest levels.

For continuous sliding, the friction between the particle and the screen is always kinetic as noted earlier. According to Garvie (1966), the kinetic friction angle between grains and screens is about 17°; thus, a kinetic friction coefficient of 0.31 was used. The friction coefficient affects the particle acceleration (equation 51), and consequently affects the absolute values of the dependent variables; however, the relationships between the dependent variables and the independent variables as well as the drive type are unchanged.

As can be noted from Chapter 3, there are seven to eight independent variables associated with screen oscillation depending on the drive used. Different value combinations of these variables give different motions of the screen and hence different motions of the particle; nevertheless, it was expected that some of the variables would have a limited effect on the motion of the particle. In order to simplify the study, the independent variables for each drive were classified depending on whether the variable was expected to have a significant effect on the particle motion or not. The variables expected to have a significant effect (the major group) are

(a) the frequency of oscillation (f),

(b) the amplitude of oscillation (A),

(c) the mean hanger angle (ϕ_m) and

(d) the screen slope angle (α).

The variables expected to have a minimal effect (the minor group) are

(a) the hanger length (R),

(b) the pitman (or connecting rod) length (L),

and for the crank-pitman drive;

(c) the initial pitman slope angle (δ_o),

and for the bent-shaft drive;

(d) the bent angle (β),

and for the spatial crank drive;

(e) the pitman length of the drive (l),

(f) the input shaft angle (β).

and for the quick-return drive;

(g) the center distance (h), and

(h) the swing-bar height/center distance ratio (e).

5.2 Program Execution

The program was run with the independent variables as its parameters or factors for each of the four drives noted previously. The values or levels for the independent variables were selected on the basis of the specifications of some commercial oscillating screens as given by Harrison and Blecha (1983); and then, trial runs were made to ensure that, for all the combinations, the particle neither rode nor hopped. After the trial runs, the program was executed with different values for the variables in the minor group (see table 1). To select the values for the other variables which were held constant, some trial runs were made to find

Table 1. Variables and Levels for the Minor Group

Variables	Levels	
Pitman length L (mm)	150	300
Hanger length R (mm)	150	250
Initial pitman angle δ_o (deg.)	0	15
Bent angle β (deg.)	25	35
Drive pitman length l (mm)	150	250
Input shaft angle β (deg.)	25	35
Center distance h (mm)	25	40
Bar/center ratio e	1.3	1.6

what values gave a high efficiency index. The following were found and subsequently used;

frequency (f) = 9 Hz,

amplitude (A) = 14 mm,

mean hanger angle (ϕ_m) = 0°, and

screen slope (α) = 10°.

An examination of the results after the trial runs showed that with two exceptions, the variables in the minor group were, as assumed, insignificant; therefore, for the remainder of the simulation they were not changed. The bent angle for the bent-shaft drive and the center distance for the quick-return drive were the two exceptions, and they appeared to have a small but systematic influence on the dependent variables. These two variables were included as the parameters with two levels for each for the following execution of the program so that their significance to particle motion could be further evaluated. The values assigned to the variables in the minor group are as follows;

hanger length (R) = 150 mm

pitman length (L) = 300 mm

and for the crank-pitman drive;

initial pitman slope angle δ_0 = 0°

and for the bent-shaft drive;

bent angle β = 25° and 35°

and for the spatial crank drive;

drive pitman length l = 150 mm

input shaft angle β = 25°

and for the quick-return drive;

center distance h = 25 mm and 40 mm

swing bar/center distance ratio e = 1.6

The program was executed again for the variables in the major group. The levels used can be seen in Table 2.

Table 2. Varibles and Levels for the Major Group

Variables	Levels		
Frequency of oscillation f (Hz)	5	7	9
Amplitude of oscillation A (mm)	6	10	14
Hanger angle ϕ (°)	0	15	
Screen slope angle α (°)	5	10	

In addition, the program was run with each of the two levels of the bent angle (β) for the bent-shaft drive and the two levels of the center distance (h) for the quick-return drive.

6. RESULTS AND DISCUSSION

6.1 Steady-pattern State of Particle Motion

The particle is initially released onto the screen with a zero velocity. Then, as noted earlier, the pattern of particle motion changes for the first few cycles of oscillation, but eventually reaches a steady state. The sequential number of the cycle during which the steady-pattern state of particle motion is reached is called the steady cycle number. The number varies with the frequency and the amplitude but is insensitive to all the other variables. For a typical example, Table 3 presents the steady cycle numbers for the crank-pitman drive.

Table 3. The Steady Cycle Number for Crank-pitman Drive

Frequency (Hz)	Amplitude (mm) 6	10	14
5	2	3	3
7	3	4	5
9	4	5	6

As can be seen from Table 3, the steady cycle number increases with the frequency and the amplitude. The rate in which it increases with the frequency is such that the time needed to reach the steady-pattern state is basically unchanged. For example, the steady cycle number increases from 2 to 4 for the amplitude of 6 mm when the frequency changes from 5 Hz to 9 Hz. The time needed to reach the steady-pattern state varies from 2/5 to 4/9 seconds, that is, slightly less than one half second. On the other hand, the increase of the steady cycle number with the amplitude means that the larger the amplitude is, the longer time is required for the particle to reach the steady-pattern state of motion.

6.2 Effects of the Independent Variables

6.2.1 Variables in the Minor Group

The average relative velocity (v_{ar}), the penetrating ratio (ϵ) and the efficiency index (EI) for all the combinations of the variables in the minor group are given in Tables 4 to 7.

For the crank-pitman drive, the pitman and the hanger lengths, and the initial pitman slope angle (L, R and δ_o) cause less than 1% change in the average relative velocity, no change at all in the penetrating ratio and a maximum change of 0.9% in the efficiency index (see Table 4).

For the bent-shaft drive, the average relative velocity has a maximum change of 1.5%. The penetrating ratio has about 6% increase but only at the smaller bent angle (25°) and the larger hanger length (250 mm) indicating that there is some interaction between the bent angle and the hanger length. The changes in the efficiency index are less than

Table 4. Average Relative Velocity, Penetrating Ratio and Efficiency Index for the Crank-pitman Drive

Pitman Length (mm)	Hanger Length (mm)	Initial Pitman Slope Angle (deg.) 0	15
		Ave. Rel. Velocity (mm/s)	
150	150	345	344
	250	343	344
300	150	346	346
	250	346	344
		Penetrating Ratio	
150	150	0.33	0.33
	250	0.33	0.33
300	150	0.33	0.33
	250	0.33	0.33
		Efficiency Index (mm/s)	
150	150	112	112
	250	111	112
300	150	113	113
	250	112	112

Table 5. Average Relative Velocity, Penetrating Ratio and Efficiency Index for the Bent-shaft Drive

Pitman Length (mm)	Hanger Length (mm)	Bent Angle (deg.) 25	35
		Ave. Rel. Velocity (mm/s)	
150	150	368	378
	250	363	372
300	150	369	376
	250	363	372
		Penetrating Ratio	
150	150	0.28	0.28
	250	0.30	0.28
300	150	0.28	0.28
	250	0.30	0.28
		Efficiency Index (mm/s)	
150	150	101	104
	250	109	102
300	150	101	103
	250	109	102

8% (see Table 5).

For the spatial crank drive, there is no change at all in the penetrating ratio and the changes in both the average relative velocity and the efficiency index are less than 1% (see Table 6).

For the quick-return drive, the maximum variation in the average relative velocity is 6% which is mainly caused by the change of the center distance h. The penetrating ratio responds also to the center distance only with a reduction of 10% when the center distance changes from 25 mm to 40 mm; however, the change in the efficiency index is less than 6% (see Table 7).

Though there seems to be some interaction between the hanger length and the bent angle and some variations occur in the dependent variables for the bent-shaft drive, the hanger length produces only very small changes (< 1[illegible]) in the dependent variables for the other three drives; therefore, its effect is generally considered unimportant. Among the variables in the minor group, only the bent angle for the bent-shaft drive and the center distance for the quick-return drive have some small but systematic influence on the dependent variables. To further evaluate their effects, the bent angle and the center distance, as mentioned earlier, were included in the parameters with two levels for each when the program was run for the major group variables. The results show that increases in either the bent angle or the center distance generally bring about

Table 6. Average Relative Velocity, Penetrating Ratio and Efficiency Index for the Spatial Crank Drive

Pitman Length (mm)	Hanger Length (mm)	Drive Pitman Length (mm) 150, Input Shaft Angle (deg.) 25	150, 35	250, 25	250, 35
		Ave. Rel. Velocity (mm/s)			
150	150	352	350	351	352
	250	350	352	349	350
300	150	352	350	351	352
	250	350	352	349	350
		Penetrating Ratio			
150	150	0.33	0.33	0.33	0.33
	250	0.33	0.33	0.33	0.33
300	150	0.33	0.33	0.33	0.33
	250	0.33	0.33	0.33	0.33
		Efficiency Index (mm/s)			
150	150	114	114	114	114
	250	114	114	113	114
300	150	114	114	114	114
	250	114	114	113	114

Table 7. Average Relative Velocity, Penetrating Ratio and Efficiency Index for the Quick-return Drive

Pitman Length (mm)	Hanger Length (mm)	Bar/Center Ratio 1.3, Center Distance (mm) 25	1.3, 40	1.6, 25	1.6, 40
		Ave. Rel. velocity (mm/s)			
150	150	248	263	253	267
	250	250	266	256	270
300	150	248	263	253	267
	250	250	266	257	270
		Penetrating Ratio			
150	150	0.48	0.43	0.48	0.43
	250	0.48	0.43	0.48	0.43
300	150	0.48	0.43	0.48	0.43
	250	0.48	0.43	0.48	0.43
		Efficiency Index (mm/s)			
150	150	118	112	120	114
	250	119	113	122	115
300	150	118	112	120	114
	250	119	113	122	115

slight increases in the average relative velocity but slight decreases in the penetrating ratio. As can be seen in Table 8 and Table 9 (the complete data are tabulated in Table B2, B3, B5 and B6 in Appendix B), the efficiency index, however, does not exhibit systematic and substantial response to either the bent angle or the center distance; therefore, the effects of the bent angle and the center

Table 8. Efficiency Index for the Bent-shaft Drive (mm/s)

Freq. (Hz)	Mean Hanger Angle (deg.)	Bent Angle (deg.)	Amplitude (mm): 6		10		14	
			Screen Slope Angle (deg.): 5	10	5	10	5	10
5	0	25	12	35	46	59	74	77
		35	15	41	54	61	73	75
	15	25	10	36	47	59	70	75
		35	16	42	55	63	75	75
7	0	25	53	57	80	80	76	95
		35	55	58	80	74	76	85
	15	25	49	56	81	76	106	91
		35	55	58	80	76	83	90
9	0	25	68	68	73	88	75	101
		35	72	71	73	86	75	103
	15	25	69	67	97	85	86	103
		35	70	67	86	82	76	99

Table 9. Efficiency Index for the Quick-return Drive (mm/s)

Freq. (Hz)	Mean Hanger Angle (deg.)	Center Dist. (mm)	Amplitude (mm): 6		10		14	
			Screen Slope Angle (deg.): 5	10	5	10	5	10
5	0	25	9	22	41	43	67	65
		40	8	23	43	44	66	63
	15	25	7	15	35	36	63	56
		40	6	16	35	39	63	56
7	0	25	48	45	76	72	106	97
		40	51	46	77	73	85	95
	15	25	44	42	74	65	76	87
		40	42	43	76	63	64	88
9	0	25	65	60	98	87	85	120
		40	66	61	91	90	81	114
	15	25	65	56	69	81	66	111
		40	66	57	67	83	61	104

distance on particle motion are considered trivial.

Generally, the independent variables in the minor group cause little or no change in the dependent variables; therefore, compared with the other independent variables whose effects will be discussed later in this Chapter, all the variables in the minor group are unimportant to particle motion.

6.2.2 Variables in the Major Group

For the four drives, the significance and the effects of the independent variables in the major group are examined from three dimensional plots (Fig. 11 to Fig. 22) which are from the data tabulated in Table B1 through Table B6 in Appendix B. For the bent-shaft drive, only the data for the bent angle of 25°, and for the quick-return drive, only the data for the center distance of 25 mm were plotted as there was little difference for the other magnitudes of the variables.

(1) *Frequency and Amplitude*

The frequency and the amplitude have the most obvious effects on the particle motion among all the independent variables. Moreover, as can be noted from the following discussion, these two variables cause similar changes in the dependent variables and also have very much the same interaction effect on each other.

The average relative velocity increases linearly with a linear increase in either the frequency or the amplitude

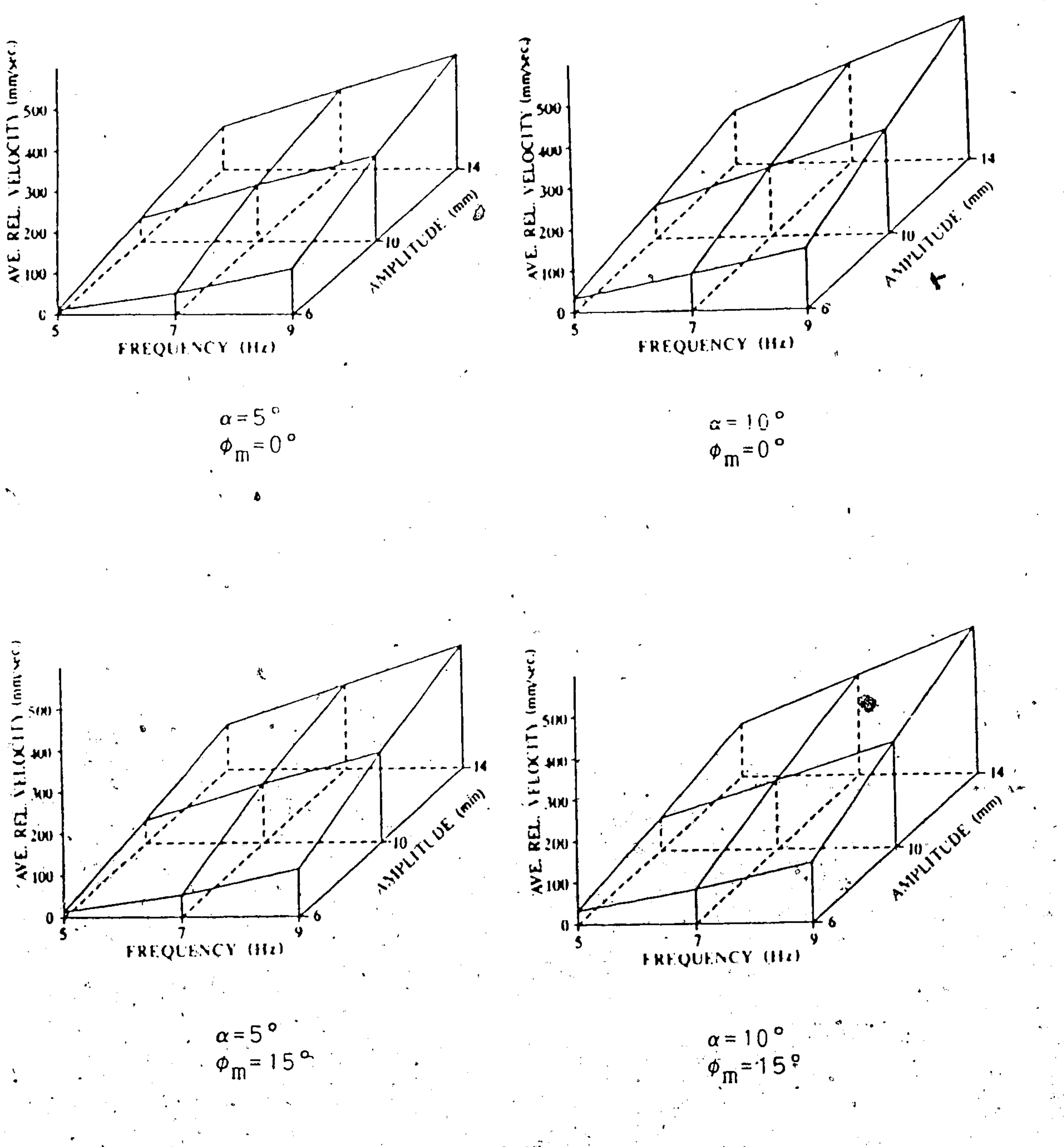

Fig. 11 Average Relative Velocity for the Crank-pitman Drive

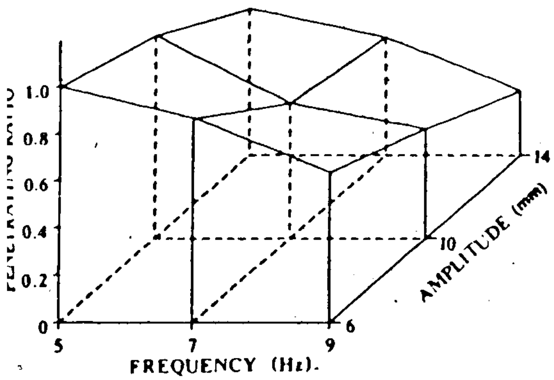

$\alpha = 5°$
$\phi_m = 0°$

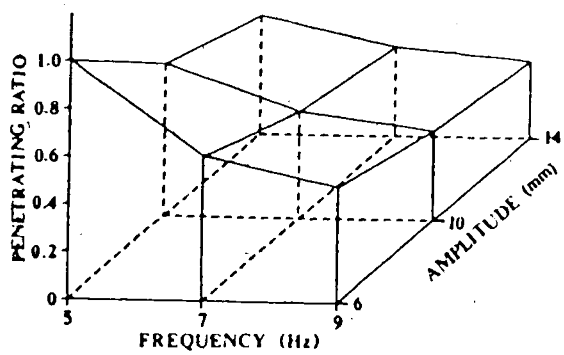

$\alpha = 10°$
$\phi_m = 0°$

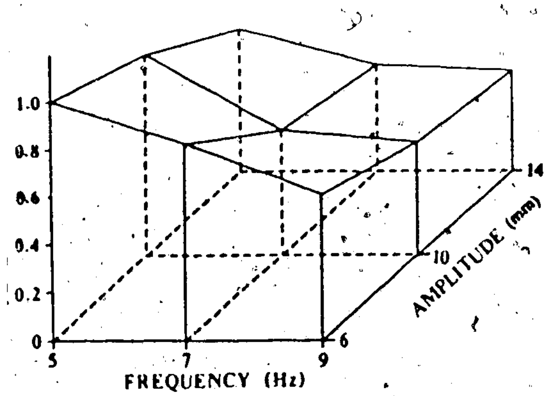

$\alpha = 5°$
$\phi_m = 15°$

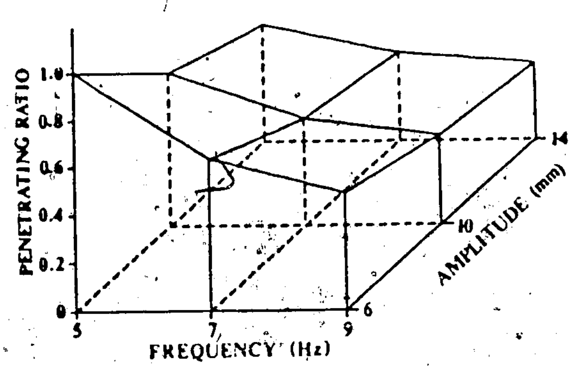

$\alpha = 10°$
$\phi_m = 15°$

Fig. 12 Penetrating Ratio for the Crank-pitman Drive

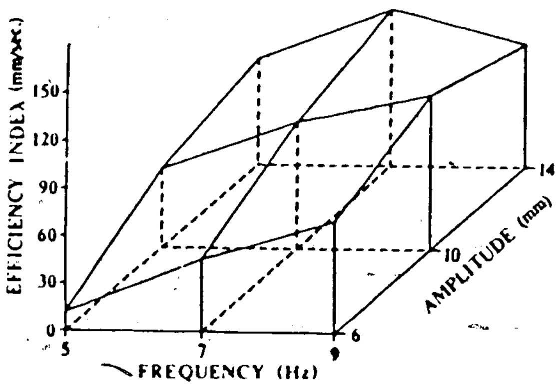

$\alpha = 5°$
$\phi_m = 0°$

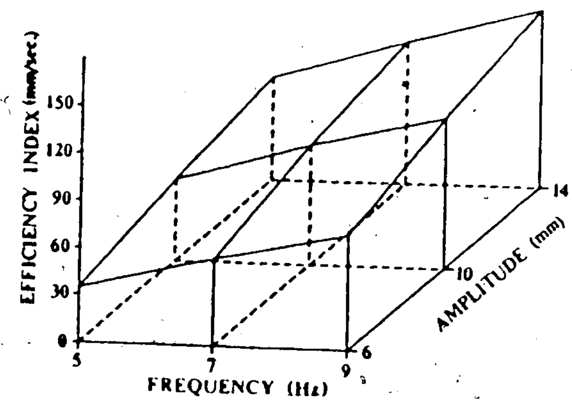

$\alpha = 10°$
$\phi_m = 0°$

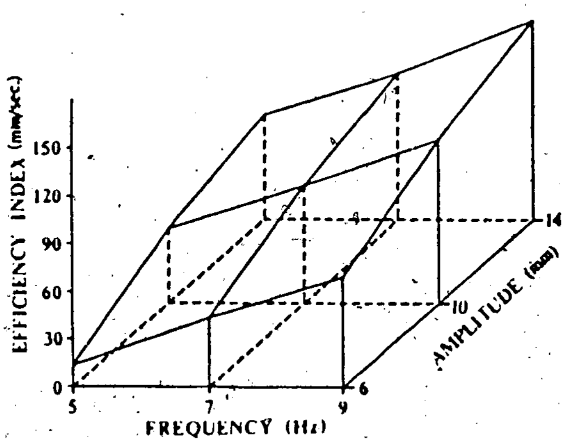

$\alpha = 5°$
$\phi_m = 15°$

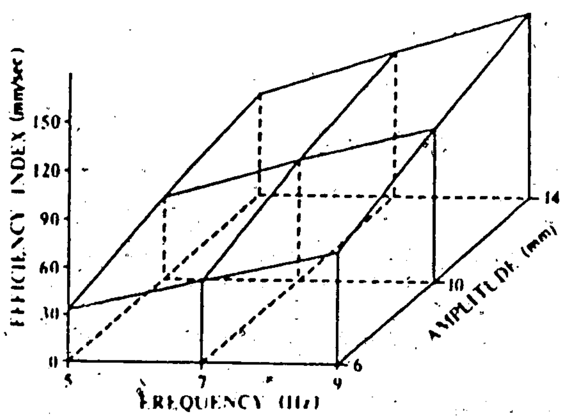

$\alpha = 10°$
$\phi_m = 15°$

Fig. 13 Efficiency Index for the Crank-pitman Drive

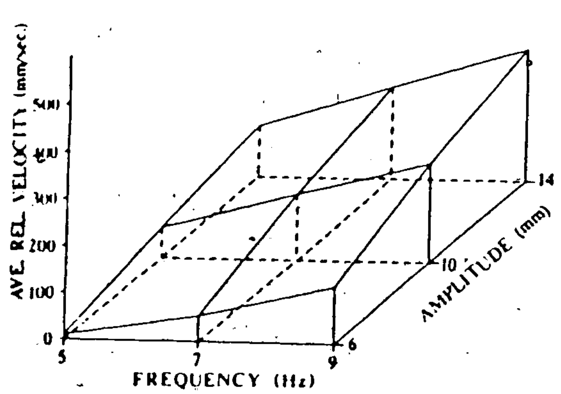

$\alpha = 5°$
$\phi_m = 0°$

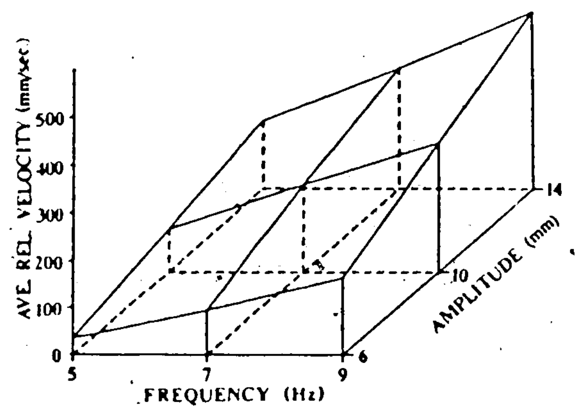

$\alpha = 10°$
$\phi_m = 0°$

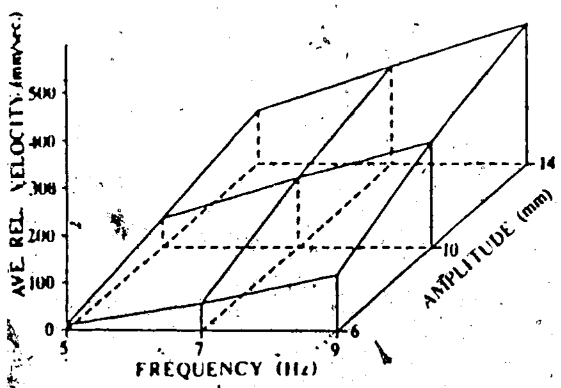

$\alpha = 5°$
$\phi_m = 15°$

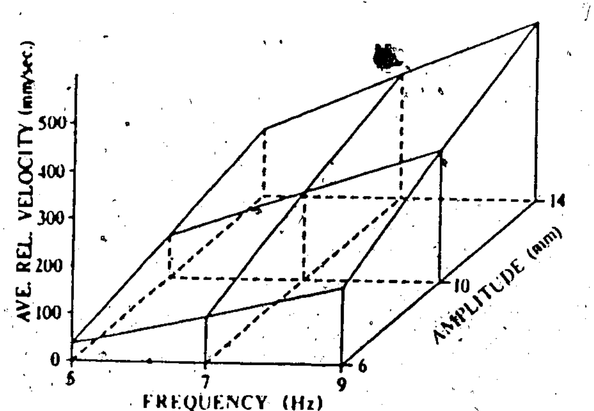

$\alpha = 10°$
$\phi_m = 15°$

Fig. 14 Average Relative Velocity for the Bent-shaft Drive

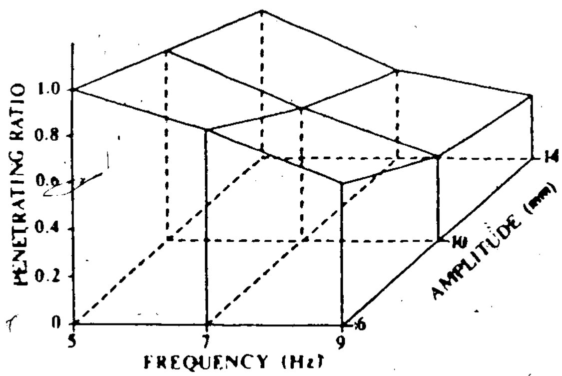

$\alpha = 5°$
$\phi_m = 0°$

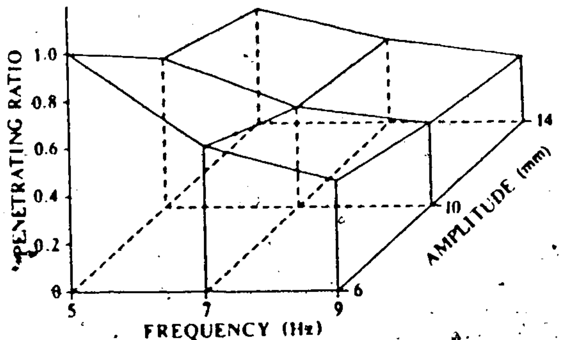

$\alpha = 10°$
$\phi_m = 0°$

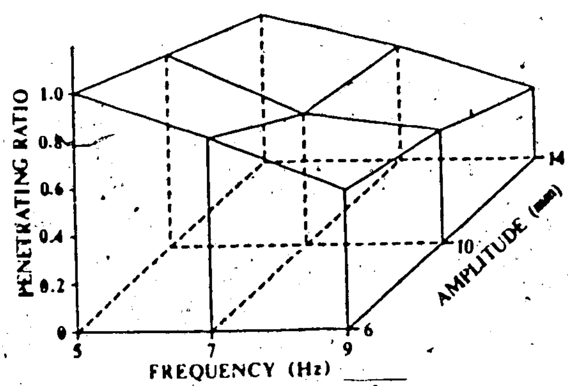

$\alpha = 5°$
$\phi_m = 15°$

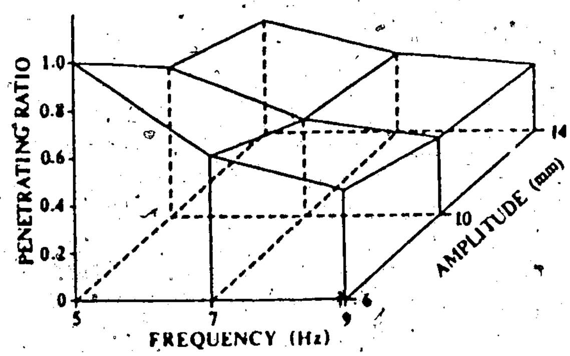

$\alpha = 10°$
$\phi_m = 15°$

Fig. 15 Penetrating Ratio for the Bent-shaft Drive

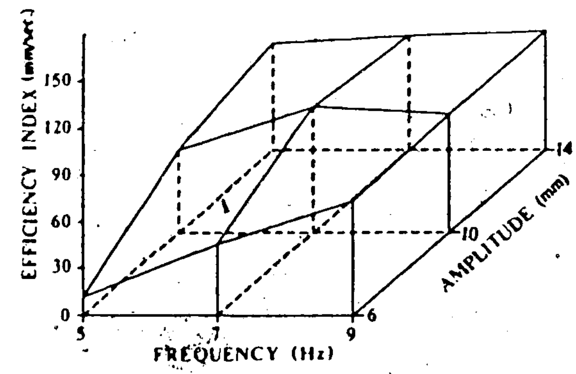

$\alpha = 5°$
$\phi_m = 0°$

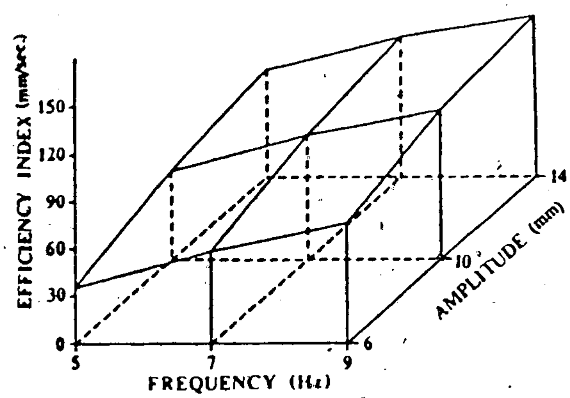

$\alpha = 10°$
$\phi_m = 0°$

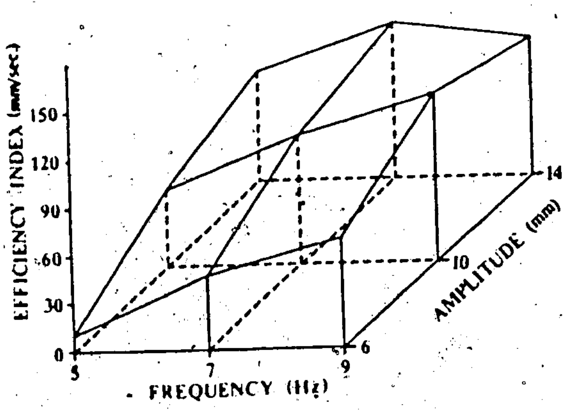

$\alpha = 5°$
$\phi_m = 15°$

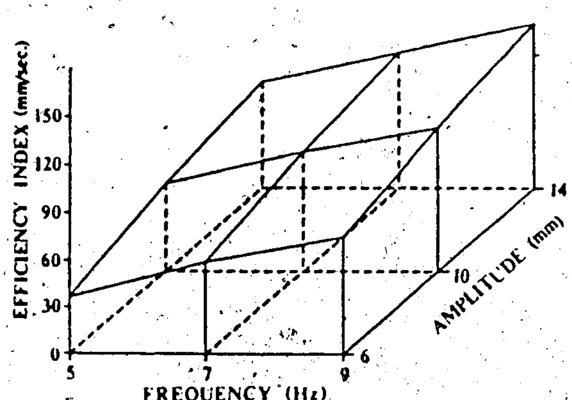

$\alpha = 10°$
$\phi_m = 15°$

Fig. 16 Efficiency Index for the
Bent-shaft Drive

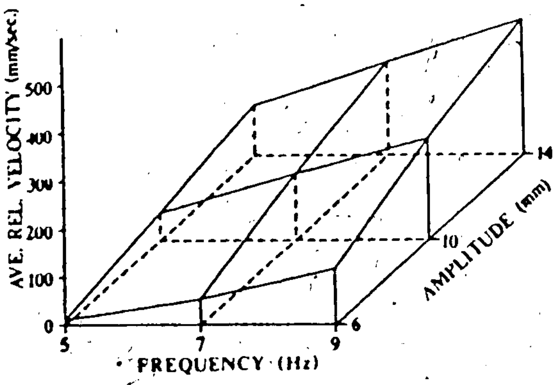

$\alpha = 5°$
$\phi_m = 0°$

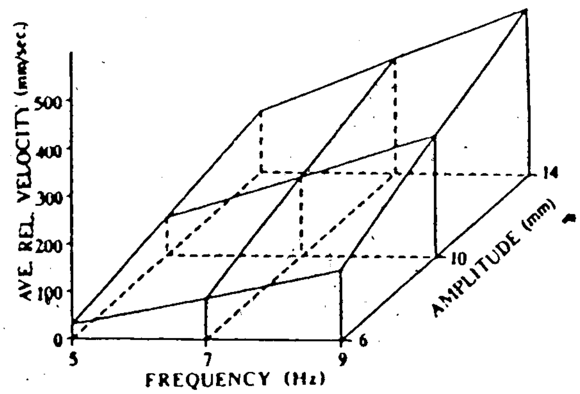

$\alpha = 10°$
$\phi_m = 0°$

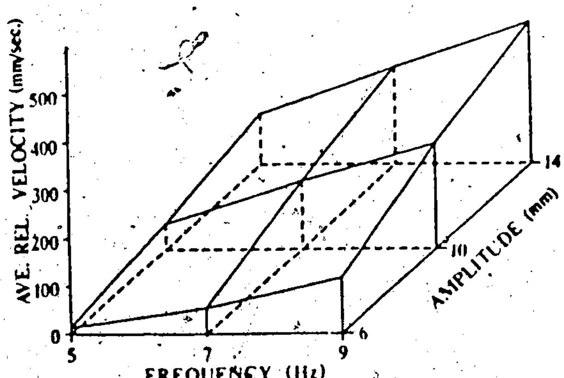

$\alpha = 5°$
$\phi_m = 15°$

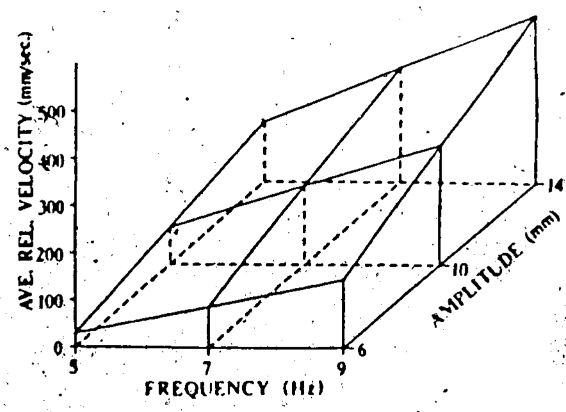

$\alpha = 10°$
$\phi_m = 15°$

Fig. 17 Average Relative Velocity for the Spatial Crank Drive

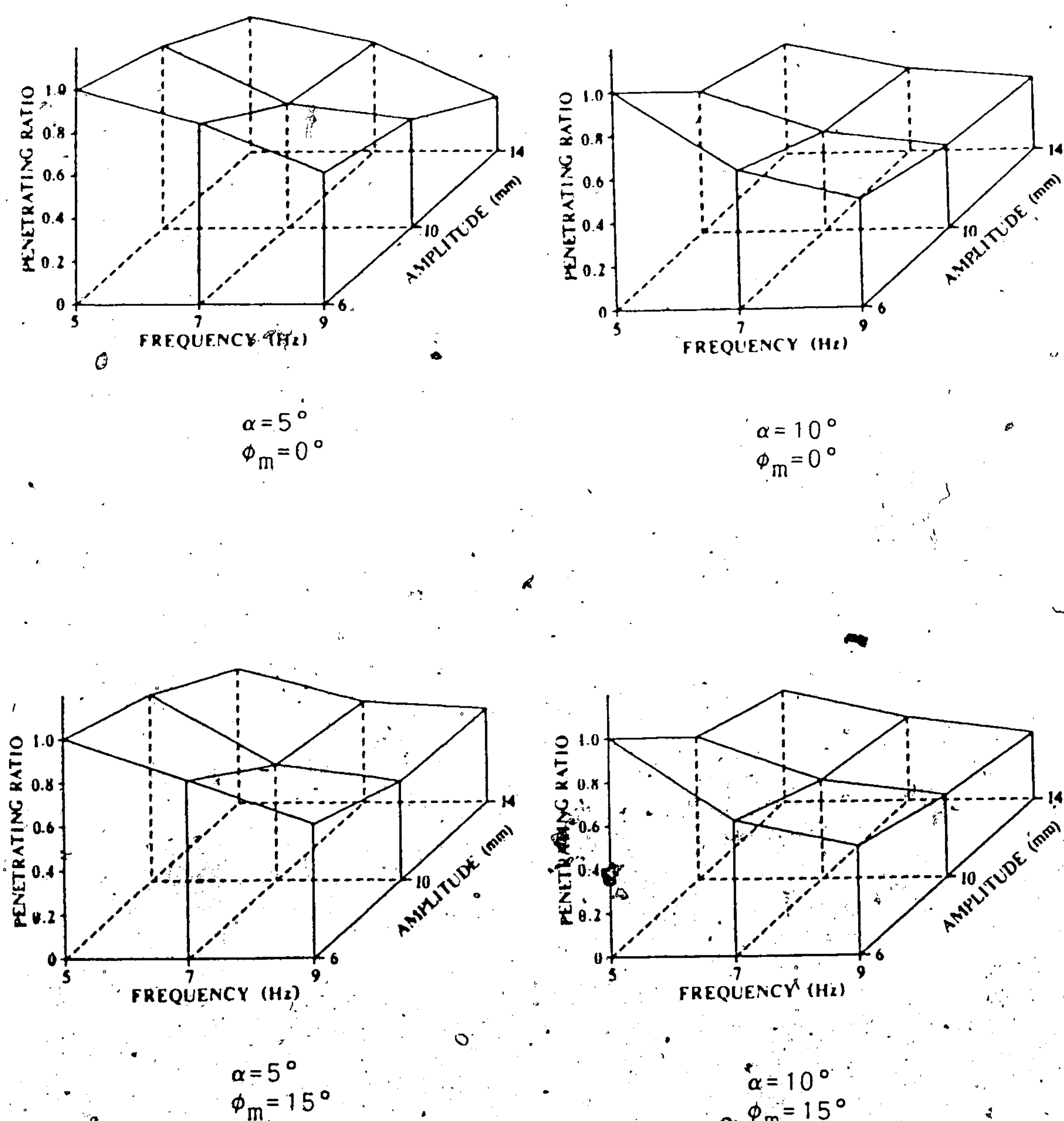

Fig. 18 Penetrating Ratio for the Spatial Crank Drive

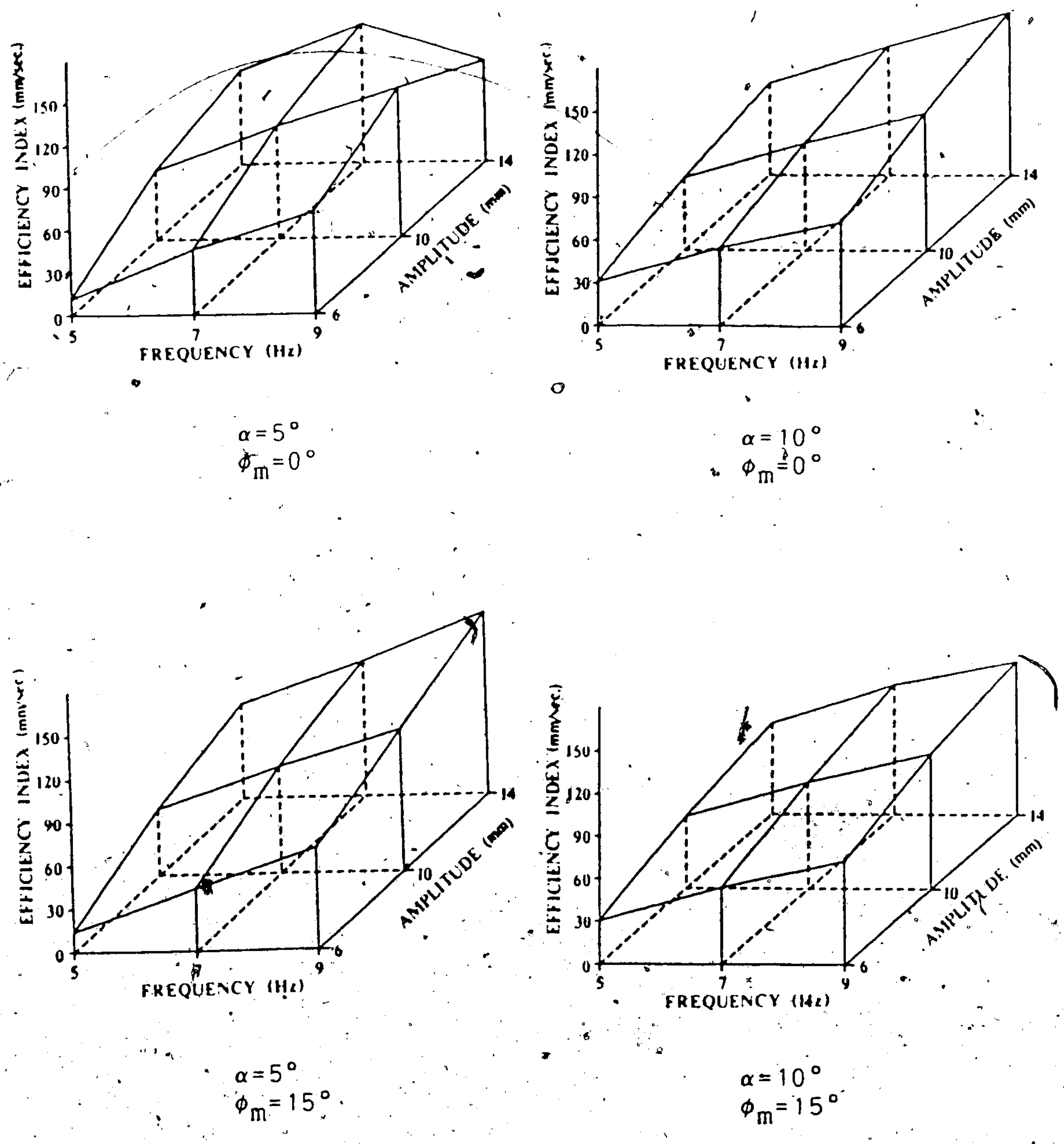

Fig. 19 Efficiency Index for the Spatial Crank Drive

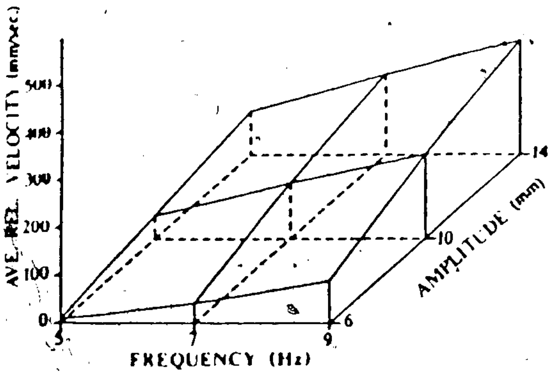

$\alpha = 5°$
$\phi_m = 0°$

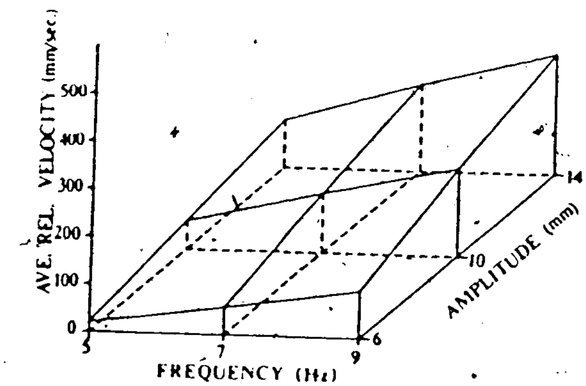

$\alpha = 10°$
$\phi_m = 0°$

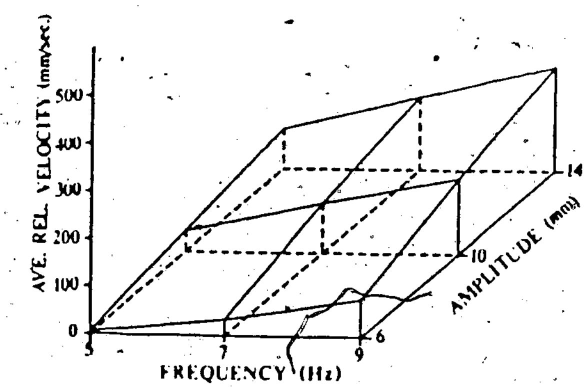

$\alpha = 5°$
$\phi_m = 15°$

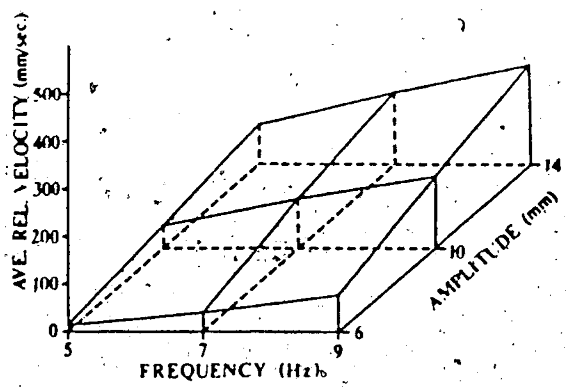

$\alpha = 10°$
$\phi_m = 15°$

Fig. 20 Average Relative Velocity for the Quick-return Drive

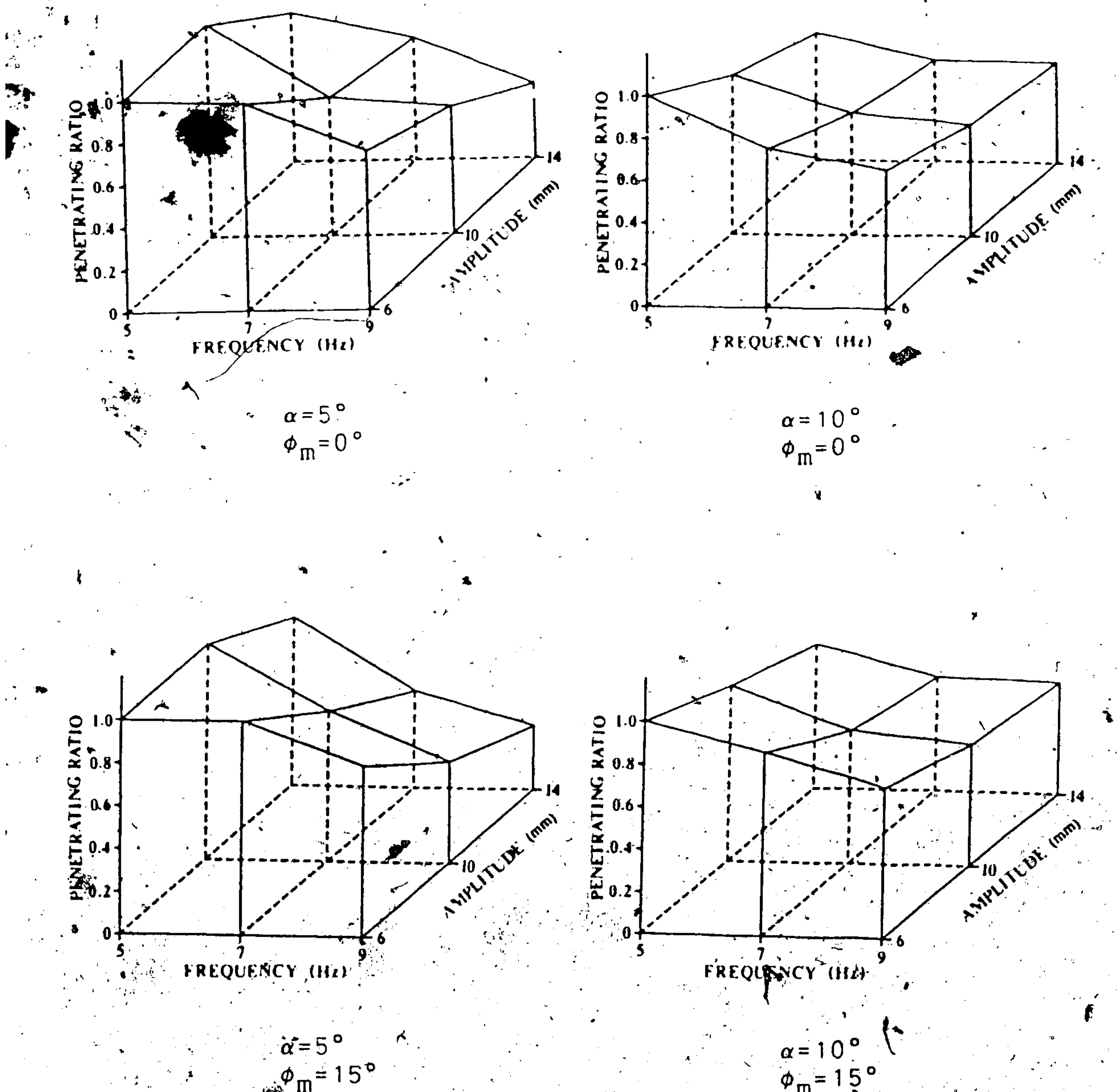

Fig. 21. Penetrating Ratio for the Quick-return Drive

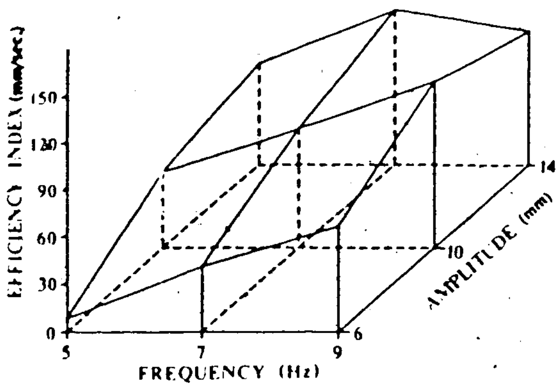

$\alpha = 5°$
$\phi_m = 0°$

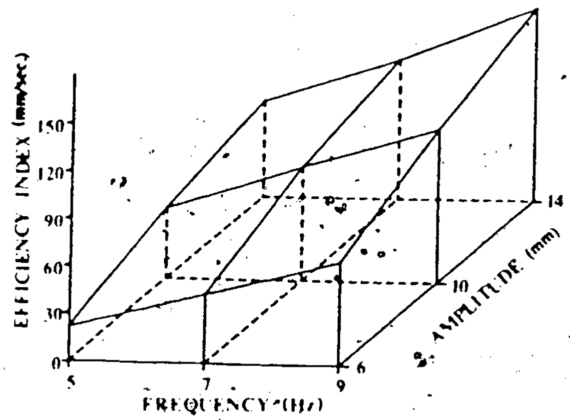

$\alpha = 10°$
$\phi_m = 0°$

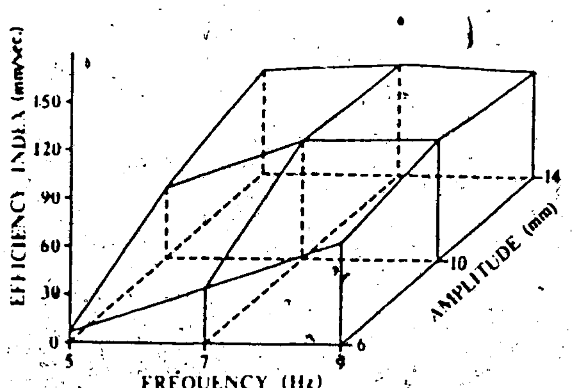

$\alpha = 5°$
$\phi_m = 15°$

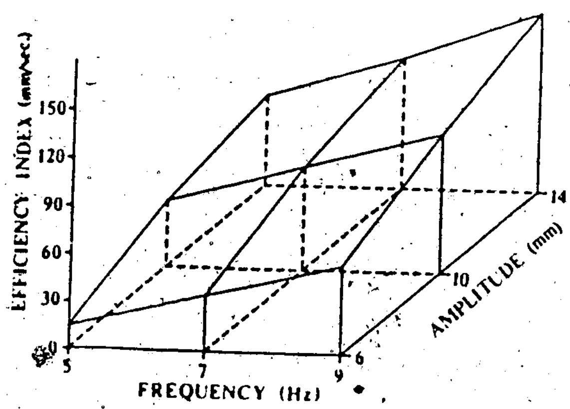

$\alpha = 10°$
$\phi_m = 15°$

Fig. 22 Efficiency Index for the Quick-return Drive for all the four drives (Fig. 11, 14, 17 and 20). Interactions between the frequency and the amplitude can be seen from the slope change of the response sufaces of the three dimensional plots. The rate at which the average relative velocity changes with one of them increases as the other one increases; in other words, the average relative velocity increases with the frequency at an increased rate if the amplitude takes a larger value, or vice versa.

With a few exceptional points, the penetrating ratio decreases curvilinearly at a decreasing rate when either the frequency or the amplitude increases. The relationship is indicated by the concave response surfaces of the plots in Fig. 12, 15, 18 and 21. Interaction exists between the frequency and the amplitude. The rate at which the penetrating ratio changes with one variable decreases if the other one takes an increased value. For example in Fig. 12 (right bottom), when the amplitude is 10 mm the penetrating ratio decreases less quickly with the fre[illegible] than it does when the amplitude is 6 mm. An interaction also exists between the frequency or the amplitude and the screen slope. For example in Fig. 18 (top left), when the screen slope angle is 5°, the penetrating ratio sometimes decreases at an increased rate at the highest levels of frequency and amplitude (f=9 Hz, A=14 mm), and when the screen slope angle is 10° it does not. The effects of the screen slope will be discussed later in this Chapter.

The effects of the frequency and the amplitude on the efficiency index are dependent of the the screen slope angle as can be seen from Fig. 13, 16, 19 and 22. For the larger screen slope (α=10°, see Fig. 22), the efficiency index increases linearly with either the frequency or the amplitude and the highest efficiency index is at the highest frequency and the largest amplitude used. There is no obvious interaction between the frequency and the amplitude. Since the efficiency index, as defined previously, is the product of the average relative velocity and the penetrating ratio, this nullification of interaction is due to the fact that the average relative velocity and the penetrating ratio have opposite responses to either the frequency or the amplitude. For the smaller screen slope (α=5°), the efficiency index increases linearly with either the frequency or the amplitude when the frequency is low or the amplitude is small; however, at high frequencies and large amplitudes, interaction between the frequency and the amplitude appears, and the efficiency index sometimes shows a decrease as either the frequency or the amplitude increases indicating that, though the efficiency index increases with the frequency and the amplitude, there exists an upper limit beyond which the efficiency index will decrease. Since the average relative velocity always increases linearly with the frequency and the amplitude, this decrease of the efficiency index is due to the sharp decrease of the penetrating ratio at high frequencies and large amplitude as noted previously. It can be seen from the discussion above that for a certain kind of material and specific screen slope and aperture size, there must be one or several frequency/amplitude combinations which give the highest efficiency index, and these combinations are dependent of the screen slope and the mean hanger angle.

(2) *Screen Slope Angle*

The effects of the screen slope angle can be evaluated by comparing the plots in the left hand column with those in the right hand column in Fig. 11 to 22. For all the four drives, the screen slope angle shows much the same effects as what are summarized below.

The effect of the gravity can be seen by varying the screen slope. Increasing the screen slope angle from 5° to 10° increases the average relative velocity, and also the rate of increase rises with the frequency and the amplitude. In other words, increasing the screen slope increases the rate at which the average relative velocity varies with the frequency and the amplitude. The relationship is typically shown by Fig. 11 in which the response surfaces of the right hand plots have higher altitudes and steeper slopes than the left hand plots.

The screen slope can affect the penetrating ratio in two ways. First, it changes the particle velocity which subsequently varies the penetrating ratio; second, it changes the limit velocities which also affect the penetrating ratio. Generally, the penetrating ratio shows a decrease with an increase in the screen slope, especially when the frequency is 7 Hz and the amplitude is 10 mm (see Fig. 15 for a typical example). As noted earlier, the screen slope interacts with the frequency and the amplitude as well as the mean hanger angle. When the screen slope angle increases from 5° to 10°, the penetrating ratio increases at the frequency of 9 Hz, the amplitude of 14 mm and the zero mean hanger angle for all the four drives (see Fig. 18).

When the screen slope angle changes from 5° to 10°, the efficiency index shows increase mainly at the lowest levels of frequency and amplitude (Fig. 13, 16, 19 and 22). At low frequencies and small amplitudes, the particle velocity relative to the screen is lower than the limit velocities (the penetrating ratio is one); then, increasing the screen slope increases the average relative velocity, and consequently, increases the efficiency index. When the penetrating ratio is less than one, increasing the screen slope does not increase the efficiency index because of the opposite responses of the average relative velocity and the penetrating ratio to the screen slope. At the highest levels of frequency and amplitude, however, the efficiency index increases with the screen slope except at the mean hanger angle of 15° for the crank-pitman and the spatial crank drives.

As can be noted from the discussion above, the effect of the screen slope is not simple because it can affect both the particle velocity and the limit velocities. Also its effect is dependent on the the frequency and the amplitude owing to its interaction with them.

(3) *Mean Hanger Angle*

The comparison of the plots in the top row with those in the bottom row in Fig. 11 through Fig. 22 shows that the significance and the effect of the mean hanger angle depend on the other variables and the drive type. When the screen slope angle is 10°, the change of the mean hanger angle from 0° to 15° does not signifcantly alter any of the three dependent variables for all the four drives. When the screen slope angle is 5°, the average velocity does not change significantly with the mean hanger angle; the penetrating ratio and the efficiency index increase only at high frequencies and large amplitudes for the crank-pitman, the bent-shaft and the spatial crank drives (Fig. 12, 13, 15, 16, 18 and 19), and decrease for the quick-return drive (Fig. 21 and 22).

Since the mean hanger angle alters the penetrating ratio only at high frequencies and large amplitudes as well as small screen slope angles, then its significance is conditional. In other words, for a specific particle-screen system, it may or may not be significant; and also its effects can differ depending on the type of the drive used. Generally, the mean hanger angle is a less important variable when compared with the frequency, the amplitude and the screen slope.

6.3 Effects of the Drives

The crank-pitman drive and the spatial crank drive give almost identical results. Apparently, these two drives impart very similar motion to the screen and consequently very similar motion to the particle. Though they give lower average relative velocities than the bent-shaft drive and smaller penetrating ratios than the quick-return drive, they give the highest efficiency indices among the four drives; therefore, in terms of the efficiency index, the crank-pitman and the spatial crank drives can be ranked first. Of course, the other factors such as the complexity of structure and the cost of manufacture also affect the feasibility of an oscillating screen drive mechanism.

The quick-return drive imparts to the screen an asymmetrical motion which has a shorter returning time. It could decrease the time when the relative velocity is higher than the limit velocity and consequently increases the penetrating ratio (Harrison and Blecha 1983). The results show that, compared with the other drives, the quick-return drive does increase the penetrating ratio considerably (Fig. 21). Among the four drives used, the quick-return drive gives the highest penetrating ratio, but the lowest average relative velocity; in consequence, the efficiency index for it is generally lower than those for the crank-pitman and the spatial crank drives. In terms of the efficiency index, the quick-return drive is then next to the crank-pitman and the spatial crank drives. For some variable combinations, however, the quick-return drive gives higher efficiency index than the crank-pitman and spatial crank drives. For example, when the frequency is 9 Hz, the amplitude is 14 mm and the mean hanger angle is zero, the quick-return drive gives efficiency indices of 85 and 120 mm/s respectively for both of the two screen slopes used, whereas the crank-pitman and the spatial crank drives give 77 and 113 mm/s, 71 and 114 mm/s respectively.

The bent-shaft drive gives the highest average relative velocity but the lowest penetrating ratio among the four drives used. The efficiency index for it turns out to be in the last place. Chen (1972) states that the bent-shaft drive generates a motion which has a lower maximum acceleration than that of a sinusoidal motion if the bent angle is larger than 5°. In this study, the bent angles used are 25° and 35°, and the bent-shaft drive does not give high efficiency index; therefore, a motion with a low maximum acceleration is not desirable for effective screening.

Compared with the traditional crank-pitman drive, the bent-shaft drive and the quick-return drive do not sufficiently improve the efficiency index; however, the bent-shaft drive gives the highest average relative velocity and the quick-return drive gives the highest penetrating ratio. The latter verifies the suggestion by Harrison and Blecha (1983) that a quick-return drive could be used to improve the penetrating ratio.

7. SUMMARY AND CONCLUSIONS

There are seven or eight variables associated with an oscillating screen depending on the drive used. According to the results of simulation, some of the variables cause very slight changes or no change at all in the dependent variables, and therefore, are considered unimportant to particle motion. Those that can substantially change the dependent variables are the significant factors to particle motion on an oscillating screen. They are

(1) the frequency of oscillation,

(2) the amplitude of oscillation and

(3) the screen slope.

The mean hanger angle causes some changes in the dependent variables only at high frequencies and large amplitudes as well as small screen slopes; therefore, its significance is conditional and its effect is dependent on the other variables.

The frequency and the amplitude of oscillation have much the same effects on particle motion and very similar effect of interaction on each other. The average relative velocity increases linearly with either the frequency or the amplitude, whereas the penetrating ratio decreases curvilinearly with either. The efficiency index generally increases when either the frequency or the amplitude increases; however, there exists an upper boundary beyond which the efficiency decreases. For a specific oscillating screen and certain kind of particles, there exist one or several combinations of frequency and amplitude which give the highest efficiency index, and these combinations are dependent on the screen slope and the mean hanger angle.

Increased screen slope gives increased average relative velocity but decreased penetrating ratio. The efficiency index shows an increase with the screen slope only at low frequencies and small amplitudes; therefore, for a specific oscillating screen and certain kind of particles, whether increasing the screen slope is beneficial to the screening efficiency depends on the frequency and the amplitude used.

The crank-pitman oscillator and the spatial crank slider impart very similar motions to the screen and to the particle. Among the driving mechanisms analyzed in this study, they give the best opportunity for particle penetration, thus, are recommendable for use as drives of oscillating screens.

Compared with the other drives, the quick-return drive can substantially increase the penetrating ratio and hence it gives a way of improving the penetrating ratio.

A motion with low maximum acceleration is not desirable for effective screening.

8. RECOMMENDATIONS

The following recommendations are made for further investigations on oscillating screens. They are;

(1) a study on oscillating screens with particles sliding and rolling,

(2) the effect of particle to particle interference on particle penetration,

(3) an experimental validation of the model so that the model can be used for design purposes.

REFERENCES

Barton, L.O. 1984. Mechanism analysis. Marcel Dekker, Inc. New York, U.S.A.

Berry, P.E. 1958. Research on oscillating conveyors. Journal of Agricultural Engineering Research 3:249-259.

Berry, P.E. 1959. Basic theory of low-acceleration oscillating conveyors. Journal of Agricultural Engineering Research 4:204-213.

Bickert, W.C. and F.H. Buelow. 1966. Kinetic friction of grains on surfaces. TRANSACTIONS of the ASAE 9(1):129-131.

Chen, P. 1972. Application of spatial mechanisms to agricultural machinery. TRANSACTIONS of the ASAE 16(2):214-217.

Edison, A.R. and W.L. Brogan. 1972. Size measurement statistics of kernels of six grains. ASAE Peper No. 72-841, ASAE, St. Joseph, MI49085.

Feller, R. and A. Foux. 1975. Oscillating screen motion effect on the particle passage through perforations. TRANSACTIONS of the ASAE 18(5):926-931.

Garvie, D.W. 1966. Operating conditions for maximum efficiency in the use of cleaning and grading machines for grain. Proc. Inst. Agric. Engrs 22(4):141-145, U.K.

Hann, S.D. and J.P. Gentry. 1970. Analysis and simulation of the motion of an ellipsoidal object on an oscillating conveyor. ASAE Peper No.70-887, ASAE, St. Joseph, MI49085.

Harrison H.P. and A. Blecha. 1983. Screen oscilation and aperture size -- sliding only. TRANSACTIONS of the ASAE 26(2):343-348.

Henderson, J.M. 1967. Measuring kinetic friction coefficients using oscillating motion. TRANSACTIONS of the ASAE 10(3):348-351.

Henderson, J.M. and A.M. Newman. 1972. Orientation of a prolate spheroid object. TRANSACTIONS of the ASAE 15(6):1128-1131.

Mofor, E.H. 1976. Motion of threshed grains on an oscillating pan. Unpublished M.Sc. thesis, Dept. of Agricultural Engineering, University of Alberta, Edmonton, Alberta.

Sampson, J.B., F. Morgan, D.W. Reed and M. Muskat. 1943. Friction behavior during the slip portion of the stick-slip process. Journal of Applied Physics. 14:689-700.

Schertz, C.E. and T.E. Hazen. 1963. Predicting motion of granular material on an oscillating conveyor. TRANSACTIONS of the ASAE 6(1):6-10.

Schertz, C.E. and T.E. Hazen. 1965. Movement of shelled corn on an oscillating conveyor. TRANSACTIONS of the ASAE 8(4):582-583.

Speckhart, F.H. and W.L. Green. 1976. A guide to using CSMP. Printice-Hall, Inc., New Jersey, U.S.A.

Turnquist, P.K. and J.G. porterfield. 1961. Four-bar links for separating and conveying. TRANSACTIONS of the ASAE 4(2):188-191.

APPENDIX A

PROGRAM LISTING

```
10 '*** SIMULATION OF PARTICLE MOTION ON AN OSCILLATING SCEEEN ***

20 '     The following program is a simulation model which predicts
22 'the motion of a particle on an oscillating screen. It calculates
24 'the screen velocity, the particle velocity, the relative particle
26 'to screen velocity, the penetrating ratio and the efficiency
28 'index when the particle is confined to continuous sliding motion.
30 'the drive type can be any one of the crank-pitman oscillator, the
32 'bent-shaft oscillator, the spatial crank slider and the
34 'quick-return oscillator. In determining the particle velocity,
36 'the Runge-Kutta fourth order integration rule is used.

40 '*** Main Section ***
45 OPEN "RESULT" FOR OUTPUT AS #1    'Open a file for output
47 PRINT "SIMULATION OF PARTICLE MOTION ON AN OSCILLATING SCREEN"
48 PRINT
50 GOSUB 230                         'Initialization of common constants
60 GOSUB 330                         'Choosing driving mechanisms
65 IF DRIVE<1 OR DRIVE>4 THEN PRINT "ILLEGAL DRIVE NUMBER":GOTO 60
67 GOSUB 1770                        'Print headings
70 GOSUB 430                         'Definition of functions
80 ON DRIVE GOSUB 470,590,700,820    'Input of system parameters
105 GOSUB 1670                       'Limit velocities & control times
107 GOSUB 930                        'Determine crank length & init. hanger angle
115 GOSUB 1850                       'Print general information
120 ON DRIVE GOSUB 1910,1950,1970,2030     'Print general information
130 GOSUB 2090                       'Print control times & sub-headings
133 '
135 'The following WHILE loop determines the particle velocity by
137 'using the Runge-Kutta fourth order integration rule.
139 '
140 WHILE TIME<=TOTIME               'Calculate system status
150   FOR COUNT=INCRMT TO OUTP STEP INCRMT
155      VPP1=VPP
160      ON DRIVE GOSUB 2150,2410,2710,3010    'Screen motion
165      ON DRIVE GOSUB 2210,2480,2790,3100    'Screen motion
170      GOSUB 3390                            'Particle acceleration
```

```
180       K1=INCRMT*APP
182       TIME=TIME+INCRMT/2
184       VPP=VPP1+K1/2
186       ON DRIVE GOSUB 2150,2410,2710,3010   'Screen motion
188       ON DRIVE GOSUB 2210,2480,2790,3100   'Screen motion
190       GOSUB 3390                           'Particle acceleration
192       K2=INCRMT*APP
194       VPP=VPP1+K2/2
196       GOSUB 3390
198       K3=INCRMT*APP
200       TIME=TIME+INCRMT/2
202       VPP=VPP1+K3
204       ON DRIVE GOSUB 2150,2410,2710,3010   'Screen motion
206       ON DRIVE GOSUB 2210,2480,2790,3100   'Screen motion
208       GOSUB 3390                           'Particle acceleration
209       K4=INCRMT*APP
210       VPP=VPP1+1/6*(K1+2*K2+2*K3+K4)       'Particle velocity
211       VRELA=VSP-VPP
212       'Check for riding mode
215       IF ABS(VRELA)<.0001 AND REC%=1 THEN LPRINT " PARTICLE RIDING, EXECUTION STOPPED."
216       IF ABS(VRELA)<.0001 AND REC%=1 THEN PRINT " PARTICLE RIDING, EXECUTION
STOPPED.":STOP
217       IF ABS(VRELA)<.0001 AND REC%=0 THEN REC%=1
218       IF ABS(VRELA)>=.0001 AND REC%=1 THEN REC%=0
219       IF STATEFLAG%=0 THEN GOSUB 3500     'Monitoring steady state
220       IF STATEFLAG%=1 THEN GOSUB 3600     'Ave. vel. & deg. of penetr.
221    NEXT COUNT
223    GOSUB 3460                        'Print system status
224 WEND
225 GOSUB 3700                           'Print ave. vel.& deg. of penetr.
226 END

230 '*** Initialization of Common Constants ***
250 PA=.0018                         'Half of the particle length, m
260 PB=.0019                         'Half of the particle height, m
270 OL=.0045                         'Opening length of screen, m
280 UK=.31                           'Kinetic coefficient of friction
```

```
285 R0=.01                              'Seed crank length
290 PI=3.14159
300 G=9.81
302 I%=1
304 DIM VRA(20), PENRTO(20)
310 CONST=PI/180
320 RETURN

330 '*** Choice of Driving Mechanisms ***
340 PRINT "PLEASE ENTER YOUR DRIVE NUMBER"
350 PRINT
360 PRINT "1. CRANK-PITMAN OSCILLATOR"
370 PRINT "2. BENT-SHAFT OSCILLATOR"
380 PRINT "3. SPATIAL CRANK-SLIDER"
390 PRINT "4. QUICK-RETURN OSCILLATOR"
400 PRINT
410 INPUT "DRIVE NUMBER = ", DRIVE
415 PRINT
420 RETURN

430 '*** Definition of Functions ***
440 DEF FNARCSIN(X)=ATN(X/SQR(1-X*X))              'Inverse sine
450 DEF FNARCCOS(X)=1.570796-ATN(X/SQR(1-X*X))     'Inverse cosine
460 RETURN

470 '*** Input of System Parameters ***

475 '--- Crank-Pitman ---.
480 PRINT "INPUT THE SYSTEM PARAMETERS FOR THE SCREEN"
490 PRINT "       WITH CRANK-PITMAN DRIVE"
560 GOSUB 850
570 INPUT "INITIAL PITMAN SLOPE ANGLE (Deg.) Delta' = ", DELTA0
575 DELTA0=DELTA0*CONST
580 RETURN

590 '--- Bent-shaft ---.
600 PRINT "INPUT THE SYSTEM PARAMETERS FOR THE SCREEN"
```

```
610 PRINT "          WITH BENT-SHAFT DRIVE"
660 GOSUB 850
680 INPUT "BENT ANGLE (Deg.) [illegible]a = ", BETA
682 BETA=BETA*CONST
690 RETURN

700 '--- Spatial Crank ---.
710 PRINT "ENTER THE SYSTEM PARAMETERS FOR THE SCREEN"
720 PRINT "      WITH SPATIAL CRANK-SLIDER DRIVE"
780 GOSUB 850
790 INPUT "DRIVE PITMAN LENGTH (m) l = ", L0
800 INPUT "INPUT SHAFT ANGLE (Deg.) Beta = ", BETA
805 BETA=BETA*CONST
810 RETURN

820 '--- Quick-Return ---.
825 PRINT "ENTER THE SYSTEM PARAMETERS FOR THE SCREEN"
830 PRINT "        WITH QUICK-RETURN DRIVE"
833 GOSUB 850
835 INPUT "CENTER DISTANCE (m) h = ", H0
840 INPUT "SWING BAR HEIGHT-CENTER DISTANCE RATIO e = ", E
842 H=E*H0
845 RETURN

850 '--- Common Parameters ---.
855 INPUT "FREQUENCY (Hz) f = ", FREQ
860 INPUT "AMPLITUDE (m) A = ", AMP
870 INPUT "HANGER ANGLE (Deg.) Phi = ", PHIMID
880 INPUT "SCREEN SLOPE ANGLE (Deg.) Alpha = ", ALPHA
885 INPUT "HANGER LENGTH (m) R = ", R
887 INPUT "PITMAN LENGTH (m) L = ", L
888 ALPHA=ALPHA*CONST
889 PHIMID=PHIMID*CONST
900 RETURN

930 '*** Determination of Crank length & Initial Hanger Angle ***
935     'according to the amplitude and hanger angle given
```

```
950 PHI0=PHIMID
960 OMEGA=2*PI*FREQ
970 TOTAL=1/FREQ
980 INTVL=TOTAL/50
990 ADIFF=.01
1000 HDIFF=.001
1003 DISCOUNT=2
1006 IF DRIVE=2 OR DRIVE=3 THEN DISCOUNT=1
1008 IF DRIVE=4 THEN DISCOUNT=4
1030 WHILE ABS(HDIFF)>.0001
1040    PHI01=PHI0
1050    PHI0=PHI0-HDIFF
1080    WHILE ABS(ADIFF)>.0001
1090       R01=R0
1100       R0=R0-ADIFF/DISCOUNT
1120       IF R0<=0! THEN R0=R01-.001
1123       IF R0<=0! THEN R0=R01-.0001
1130       ON DRIVE GOSUB 1435,1490,1550,1610
1150       T=SQR(W^2+Z^2)
1160       LAMBDA=ATN(W/Z)
1170       TIME=0!
1180       MAXPHI=PHI0
1190       MINPHI=PHI0
1200       FOR COUNT=0! TO TOTAL STEP INTVL
1240         ON DRIVE GOSUB 2150,2410,2710,3010
1250         IF PHI>MAXPHI THEN MAXPHI=PHI
1260         IF PHI<MINPHI THEN MINPHI=PHI
1270         TIME=TIME+INTVL
1280       NEXT COUNT
1290       PHISPAN=MAXPHI-MINPHI
1295       TRUEAMP=R*PHISPAN
1300       ADIFF=TRUEAMP-AMP
1310       HANGLE=(MAXPHI+MINPHI)/2
1315       HDIFF=HANGLE-PHIMID
1330    WEND
1350    ADIFF1=ADIFF
1360    ADIFF=.00011
```

```
1370 WEND
1375 TIME=0!
1420 RETURN

1430 '*** Calculation of System Constants ***

1435 '--- Crank-Pitman ---.
1440 W=L*COS(DELTA0)-R*SIN(PHI0)-R0*SIN(DELTA0)
1450 Z=L*SIN(DELTA0)+R*COS(PHI0)+R0*COS(DELTA0)
1480 RETURN

1490 '--- Bent-Shaft ---.
1500 W=L-R*SIN(PHI0)
1510 Z=R0+R*COS(PHI0)
1540 RETURN

1550 '--- Spatial Crank ---.
1560 W=L-R*SIN(PHI0)
1570 Z=R*COS(PHI0)
1600 RETURN

1610 '--- Quick-Return ---.
1620 W=L-R*SIN(PHI0)
1630 Z=H+R*COS(PHI0)
1660 RETURN

1670 '*** Limit Velocity and Control Times ***
1680 'Up Slope Limit Velocity
1690 ULV=SQR(2*PA/(G*COS(ALPHA)))*((OL-PB)/(2*PA)*G*COS(ALPHA)+.5*G*SIN(ALPHA))
1700 'Down Slope Limit Velocity
1710 DLV=SQR(2*PA/(G*COS(ALPHA)))*((OL-PB)/(2*PA)*G*COS(ALPHA)-.5*G*SIN(ALPHA))
1715 PRINT
1720 INPUT "TOTAL RUN TIME IN SEC. = ", TOTIME
1730 INPUT "INITIAL PARTICLE VELOCITY IN M/SEC. = ", VPP
1735 PERIOD=1/FREQ
1740 INCRMT=PERIOD/40
1750 OUTP=PERIOD/20
```

```
1760 RETURN

1770 '*** Print Headings ***
1775 LPRINT "SIMULATION OF PARTICLE MOTION ON AN OSCILLATING SCREEN"
1777 LPRINT
1780 ON DRIVE GOSUB 1830,1832,1834,1836
1828 RETURN
1830 LPRINT TAB(18)"Drive: Crank-Pitman"
1831 RETURN
1832 LPRINT TAB(18)"Drive: Bent-Shaft"
1833 RETURN
1834 LPRINT TAB(18)"Drive: Spatial-Crank"
1835 RETURN
1836 LPRINT TAB(18)"Drive: Quick-Return"
1837 RETURN

1840 '*** Print Parameter Values Chosen ***

1850 '--- Common Parameters ---.
1855 LPRINT
1860 LPRINT " Frequency:            ", FREQ,        "Hz"
1870 LPRINT " Amplitude:            ", AMP,         "m"
1880 LPRINT " Hanger angle:         ", PHIMID/CONST,"Deg."
1890 LPRINT " Screen slope angle:   ", ALPHA/CONST, "Deg."
1893 LPRINT
1895 LPRINT " Hanger length:        ", R,           "m"
1898 LPRINT " Pitman length:        ", L,           "m"
1900 RETURN

1910 '--- Crank-Pitman ---.
1915 LPRINT " Initi. pitman slope: ", DELTA0/CONST,"Deg."
1920 RETURN

1950 '--- Bent-Shaft ---.
1955 LPRINT " Bent angle:           ", BETA/CONST,  "Deg."
1960 RETURN
```

```
1970 '--- Spatial-Crank ---.
1980 LPRINT " Drive pitman length: ", L0,            "m"
1990 LPRINT " Input shaft angle:   ", BETA/CONST,    "Deg."
2020 RETURN

2030 '--- Quick-Return ---.
2040 LPRINT " Center distance:     ", H0,            "m"
2050 LPRINT " Bar height/C.D. ratio:", E
2080 RETURN

2090 '*** Print Control Times & Sub-headings ***
2091 LPRINT
2092 LPRINT " Step length:         ", INCRMT,    "sec."
2093 LPRINT " Output interval:     ", OUTP,      "sec."
2094 LPRINT " Total run time:      ", TOTIME,    "sec."
2095 LPRINT
2100 PRINT
2110 PRINT "  Time      Screen Vel.  Particle Vel.   Vs-Vp"
2114 LPRINT
2118 'LPRINT "  Time      Screen Vel.  Particle Vel.   Vs-Vp"
2120 RETURN

2130 '*** Motion of Screen ***

2140 '--- Crank-Pitman ---.
2150 '        <1>
2160 ETA=LAMBDA-OMEGA*TIME+DELTA0
2170 M=SQR(T^2+R0^2-2*T*R0*COS(ETA))
2180 GAMMA=FNARCSIN(R0/M*SIN(ETA))
2190 PHI=FNARCCOS((R^2+M^2-L^2)/(2*R*M))-LAMBDA-GAMMA
2200 RETURN
2210 '        <2>
2220 PSI=FNARCCOS((L^2+R^2-M^2)/(2*L*R))
2230 DELTA=PSI-PI/2+PHI
2240 VE=OMEGA*R0
2250 VSE=SIN(OMEGA*TIME-DELTA0+PHI)/COS(PHI-DELTA)*VE
2260 VS=COS(OMEGA*TIME+DELTA-DELTA0)/COS(PHI-DELTA)*VE
```

```
2270 VSP=VS*COS(PHI+ALPHA)
2280 VSV=VS*SIN(PHI+ALPHA)
2290 A1=COS(PHI)
2300 A2=-SIN(PHI)
2310 B1=SIN(DELTA)
2320 B2=COS(DELTA)
2330 C1=VS^2/R*SIN(PHI)-OMEGA^2*R0*SIN(OMEGA*TIME-DELTA0)-VSE^2/L*COS(DELTA)
2340 C2=VS^2/R*COS(PHI)+OMEGA^2*R0*COS(OMEGA*TIME-DELTA0)+VSE^2/L*SIN(DELTA)
2350 AST=(C1*B2-C2*B1)/(A1*B2-A2*B1)
2360 ASN=VS^2/R
2370 ASP=AST*COS(PHI+ALPHA)-ASN*SIN(PHI+ALPHA)
2380 ASV=AST*SIN(PHI+ALPHA)+ASN*COS(PHI+ALPHA)
2390 RETURN

2400 '--- Bent-Shaft ---.
2410 '       <1>
2420 THETA=ATN(TAN(BETA)*SIN(OMEGA*TIME))
2430 ETA=LAMBDA-THETA
2440 M=(T^2+R0^2-2*T*R0*COS(ETA))^.5
2450 GAMMA=FNARCSIN(R0/M*SIN(ETA))
2460 PHI=FNARCCOS((R^2+M^2-L^2)/(2*R*M))-LAMBDA-GAMMA
2470 RETURN
2480 '       <2>
2490 PSI=FNARCCOS((R^2+L^2-M^2)/(2*R*L))
2500 DELTA=PSI-PI/2+PHI
2510 VE=(R0*OMEGA*TAN(BETA)*COS(OMEGA*TIME))/(1+(TAN(BETA))^2*(SIN(OMEGA*TIME))^2)
2520 VSE=SIN(THETA+PHI)/COS(PHI-DELTA)*VE
2530 VS=COS(DELTA+THETA)/COS(PHI-DELTA)*VE
2540 VSP=VS*COS(PHI+ALPHA)
2550 VSV=VS*SIN(PHI+ALPHA)
2560 AETNU=-R0*OMEGA^2*TAN(BETA)*SIN(OMEGA*TIME)*(1+(TAN(BETA))^2*(1+(COS(OMEGA*TIME))^2))
2570 AETDE=(1+(TAN(BETA))^2*(SIN(OMEGA*TIME))^2)^2
2580 AET=AETNU/AETDE
2590 A1=COS(PHI)
2600 A2=-SIN(PHI)
2610 B1=SIN(DELTA)
2620 B2=COS(DELTA)
```

```
2630 C1=VS^2/R*SIN(PHI)-VE^2/R0*SIN(THETA)+AET*COS(THETA)-VSE^2/L*COS(DELTA)
2640 C2=VS^2/R*COS(PHI)+VE^2/R0*COS(THETA)+AET*SIN(THETA)+VSE^2/L*SIN(DELTA)
2650 AST=(C1*B2-C2*B1)/(A1*B2-A2*B1)
2660 ASN=VS^2/R
2670 ASP=AST*COS(PHI+ALPHA)-ASN*SIN(PHI+ALPHA)
2680 ASV=AST*SIN(PHI+ALPHA)+ASN*COS(PHI+ALPHA)
2690 RETURN

2700 '--- Spatial-Crank ---
2710 '        <1>
2720 F0=R0*SIN(BETA)*SIN(OMEGA*TIME)
2730 U0=(L0^2-R0^2+F0^2)^.5
2740 XE=U0+F0-(L0^2-R0^2)^.5
2750 M=(T^2+XE^2-2*T*XE*SIN(LAMBDA))^.5
2760 GAMMA=FNARCSIN(XE/M*COS(LAMBDA))
2770 PHI=FNARCCOS((R^2+M^2-L^2)/(2*R*M))-LAMBDA+GAMMA
2780 RETURN
2790 '        <2>
2800 PSI=FNARCCOS((R^2+L^2-M^2)/(2*R*L))
2810 DELTA=PSI-PI/2+PHI
2820 K0=R0*SIN(BETA)*COS(OMEGA*TIME)
2830 VE=(F0/U0+1)*K0*OMEGA
2840 VSE=SIN(PHI)/COS(PHI-DELTA)*VE
2850 VS=COS(DELTA)/COS(PHI-DELTA)*VE
2860 VSP=VS*COS(PHI+ALPHA)
2870 VSV=VS*SIN(PHI+ALPHA)
2880 AET=-(F0*(F0/U0+1)-K0^2/U0*(F0^2/U0^2-1))*OMEGA^2
2890 A1=COS(PHI)
2900 A2=-SIN(PHI)
2910 B1=SIN(DELTA)
2920 B2=COS(DELTA)
2930 C1=VS^2/R*SIN(PHI)+AET-VSE^2/L*COS(DELTA)
2940 C2=VS^2/R*COS(PHI)+VSE^2/L*SIN(DELTA)
2950 AST=(C1*B2-C2*B1)/(A1*B2-A2*B1)
2960 ASN=VS^2/R
2970 ASP=AST*COS(PHI+ALPHA)-ASN*SIN(PHI+ALPHA)
2980 ASV=AST*SIN(PHI+ALPHA)+ASN*COS(PHI+ALPHA)
```

```
2990 RETURN
3000 '--- Quick-Return ---.
3010 '      <1>
3015 L0=SQR(R0^2+H0^2+2*R0*H0*COS(OMEGA*TIME))
3040 THETA=FNARCSIN(R0/L0*SIN(OMEGA*TIME))
3050 ETA=LAMBDA-THETA
3060 M=SQR(T^2+H^2-2*T*H*COS(ETA))
3070 GAMMA=FNARCSIN(H/M*SIN(ETA))
3080 PHI=FNARCCOS((R^2+M^2-L^2)/(2*R*M))-LAMBDA-GAMMA
3090 RETURN
3100 '      <2>
3110 PSI=FNARCCOS((R^2+L^2-M^2)/(2*R*L))
3120 DELTA=PSI-PI/2+PHI
3130 VB1=OMEGA*R0*COS(OMEGA*TIME-THETA)
3140 VBB1=OMEGA*R0*SIN(OMEGA*TIME-THETA)
3150 VE=H/L0*VB1
3160 VSE=SIN(THETA+PHI)/COS(PHI-DELTA)*VE
3170 VS=COS(DELTA+THETA)/COS(PHI-DELTA)*VE
3180 VSP=VS*COS(PHI+ALPHA)
3190 VSV=VS*SIN(PHI+ALPHA)
3200 AA1=COS(THETA)
3210 AA2=SIN(THETA)
3220 BB1=-SIN(THETA)
3230 BB2=COS(THETA)
3240 CC1=VB1^2/L0*SIN(THETA)+2*VBB1*VB1/L0*COS(THETA)-OMEGA^2*R0*SIN(OMEGA*TIME)
3250 CC2=-VB1^2/L0*COS(THETA)+2*VBB1*VB1/L0*SIN(THETA)+OMEGA^2*R0*COS(OMEGA*TIME)
3260 AB1T=(CC1*BB2-CC2*BB1)/(AA1*BB2-AA2*BB1)
3270 AET=H/L0*AB1T
3280 A1=COS(PHI)
3290 A2=-SIN(PHI)
3300 B1=SIN(DELTA)
3310 B2=COS(DELTA)
3320 C1=VS^2/R*SIN(PHI)-VE^2/H*SIN(THETA)+AET*COS(THETA)-VSE^2/L*COS(DELTA)
3330 C2=VS^2/R*COS(PHI)+VE^2/H*COS(THETA)+AET*SIN(THETA)+VSE^2/L*SIN(DELTA)
3340 AST=(C1*B2-C2*B1)/(A1*B2-A2*B1)
3350 ASN=VS^2/R
```

```
3360 ASP=AST*COS(PHI+ALPHA)-ASN*SIN(PHI+ALPHA)
3370 ASV=AST*SIN(PHI+ALPHA)+ASN*COS(PHI+ALPHA)
3380 RETURN

3390 '*** Acceleration of Particle ***
3392 AVER=AST*SIN(PHI)+ASN*COS(PHI)
3393 IF AVER<-G THEN LPRINT " PARTICLE HOPPING, EXECUTION STOPPED."
3394 IF AVER<-G THEN PRINT " PARTICLE HOPPING, EXECUTION STOPPED.":STOP
3400 APP=SGN(VSP-VPP)*UK*(ASV+G*COS(ALPHA))+G*SIN(ALPHA)
3450 RETURN

3460 '*** Print System Status ***
3470 PRINT USING "##.######    ";TIME;VSP;VPP;VRELA
3480 PRINT #1, USING "##.######    ";TIME;VSP;VPP;VRELA
3490 RETURN

3500 '*** Monitoring of Steady State ***
3510 VSUM=VSUM+ABS(VPP)
3520 NUM=NUM+1
3530 POINTER=POINTER+INCRMT
3540 IF POINTER>=PERIOD THEN VAVE=VSUM/NUM:LOCATE ,53:PRINT
VAVE:NUM=0!:POINTER=0!:VSUM=0!:CYCL=CYCL+1
3550 IF ABS(VAVE-VAVE1)<.005 AND VAVE*VAVE1<>0! THEN STATEFLAG%=1
3553 IF STATEFLAG%=0 AND VAVE<>0! THEN VAVE1=VAVE:VAVE=0
3555 IF STATEFLAG%=1 THEN PRINT " STEADY STATE REACHED AT CYCLE";CYCL
3558 IF STATEFLAG%=1 THEN LPRINT " STEADY STATE REACHED AT CYCLE";CYCL
3560 RETURN

3600 '*** Ave. Vel. & Penetrating Ratio ***
3610 VRSUM=VRSUM+ABS(VRELA)
3620 FIGURE=FIGURE+1
3630 CLOCK=CLOCK+INCRMT
3640 IF VRELA>=0! AND VRELA<ULV THEN PASS=PASS+1
3650 IF VRELA<0! AND ABS(VRELA)<DLV THEN PASS=PASS+1
3660 IF CLOCK>=PERIOD THEN VRAVE=VRSUM/FIGURE:VRA(I%)=VRAVE
3670 IF CLOCK>=PERIOD THEN PR=PASS/FIGURE:PENRTO(I%)=PR
3680 IF CLOCK>=PERIOD THEN VRSUM=0!:FIGURE=0!:CLOCK=0!:I%=I%+1:PASS=0!
```

```
3690 RETURN

3700 '*** Print Ave. Vel. & Penetr. Ratio ***
3705 I%=I%-1
3706 PRINT
3707 PRINT " AVE. VEL.(m/s)   PENETR. RATIO"
3708 LPRINT
3709 LPRINT " AVE. VEL.(m/s)   PENETR. RATIO"
3710 FOR KK%=1 TO I%
3720    VARRAYS=VARRAYS+VRA(KK%)
3730    PRSUM=PRSUM+PENRTO(KK%)
3740    PRINT USING "   ##.#####     ";VRA(KK%);PENRTO(KK%)
3750    LPRINT USING "   ##.#####     ";VRA(KK%);PENRTO(KK%)
3760 NEXT KK%
3770 VRELAAVE=VARRAYS/I%
3780 PENETRATIO=PRSUM/I%
3785 EFFINDEX=VRELAAVE*PENETRATIO
3790 PRINT
3800 PRINT " AVERAGE RELATIVE VELOCITY = ";VRELAAVE
3810 PRINT " PENETRATING RATIO = ";PENETRATIO
3815 PRINT " EFFICIENCY INDEX = ";EFFINDEX
3820 LPRINT
3830 LPRINT " AVERAGE RELATIVE VELOCITY = ";VRELAAVE
3840 LPRINT " PENETRATING RATIO = ";PENETRATIO
3845 LPRINT " EFFICIENCY INDEX = ";EFFINDEX
3850 RETURN
```

APPENDIX B

OUTPUT DATA FOR THE AVERAGE RELATIVE VELOCITY, THE PENETRATING RATIO AND THE EFFICIENCY INDEX

Table B1. Average Relative Velocity, Penetrating Ratio and Efficiency Index for the Crank-pitman Drive

Freq. (Hz)	Mean Hanger Angle (deg.)	Amplitude (mm) 6		10		14	
		Screen Slope Angle (deg.) 5	10	5	10	5	10
		Ave. Rel. Velocity (mm/s)					
5	0	12	35	53	91	111	149
	15	14	33	53	83	115	145
7	0	58	81	139	169	210	246
	15	55	79	142	167	217	256
9	0	107	131	195	240	279	346
	15	108	128	204	242	295	356
		Penetrating Ratio					
5	0	1.0	1.0	0.87	0.61	0.63	0.49
	15	1.0	1.0	0.82	0.63	0.61	0.49
7	0	0.86	0.64	0.58	0.45	0.47	0.38
	15	0.85	0.65	0.53	0.45	0.48	0.38
9	0	0.63	0.50	0.50	0.38	0.28	0.33
	15	0.61	0.50	0.45	0.38	0.43	0.33
		Efficiency Index (mm/s)					
5	0	12	35	46	55	71	73
	15	14	33	44	53	70	71
7	0	50	52	80	76	98	95
	15	47	51	75	75	103	96
9	0	67	65	98	90	77	113
	15	66	64	92	91	126	116

Table B2. Average Relative Velocity, Penetrating Ratio and Efficiency Index for the Bent-shaft Drive
Bent angle β=25°

Freq. (Hz)	Mean Hanger Angle (deg.)	Amplitude (mm) 6		10		14	
		Screen Slope Angle (deg.) 5	10	5	10	5	10
		Ave. Rel. Velocity (mm/s)					
5	0	11	35	55	96	123	166
	15	10	36	58	97	119	162
7	0	65	91	142	185	210	272
	15	60	89	148	187	222	279
9	0	108	142	193	252	278	369
	15	112	142	204	262	295	376
		Penetrating Ratio					
5	0	1.0	1.0	0.83	0.61	0.60	0.46
	15	1.0	1.0	0.81	0.61	0.59	0.46
7	0	0.81	0.63	0.57	0.42	0.36	0.35
	15	0.80	0.63	0.55	0.41	0.48	0.33
9	0	0.63	0.48	0.38	0.35	0.27	0.28
	15	0.61	0.47	0.48	0.33	0.29	0.28
		Efficiency Index (mm/s)					
5	0	12	35	46	59	74	77
	15	10	36	47	59	70	75
7	0	53	57	80	80	76	95
	15	49	56	81	76	106	91
9	0	68	68	73	88	75	101
	15	69	67	97	85	86	103

Table B3. Average Realtive Velocity, Penetrating Ratio and Efficiency Index for the Bent-shaft Drive
Bent angle β=35°

	Mean	Amplitude (mm)					
	Hanger	6		10		14	
Freq.	Angle	Screen Slope Angle (deg.)					
(Hz)	(deg.)	5	10	5	10	5	10
		Ave. Rel. Velocity (mm/s)					
5	0	15	42	69	111	130	184
	15	16	45	72	107	136	188
7	0	70	104	145	198	211	284
	15	71	101	152	203	222	300
9	0	111	150	195	266	275	376
	15	117	157	206	275	292	396
		Penetrating Ratio					
5	0	1.0	0.98	0.78	0.55	0.56	0.41
	15	1.0	0.93	0.76	0.59	0.55	0.40
7	0	0.79	0.55	0.55	0.38	0.36	0.30
	15	0.77	0.58	0.53	0.38	0.38	0.30
9	0	0.65	0.48	0.38	0.33	0.27	0.28
	15	0.60	0.43	0.42	0.30	0.26	0.25
		Efficiency Index (mm/s)					
5	0	15	41	54	60	73	75
	15	16	42	55	63	75	75
7	0	55	58	80	84	76	85
	15	55	58	80	76	83	90
9	0	72	71	73	86	75	103
	15	70	67	86	82	76	99

Table B4. Average Relative Velocity, Penetrating Ratio and Efficiency Index for the Saptial Crank Drive

Freq. (Hz)	Mean Hanger Angle (deg.)	Amplitude (mm) 6, Screen Slope Angle (deg.) 5	6, 10	10, 5	10, 10	14, 5	14, 10
		Ave. Rel. Velocity (mm/s)					
5	0	12	31	55	87	118	148
	15	14	30	54	87	117	145
7	0	58	79	139	168	211	259
	15	54	79	142	169	220	256
9	0	106	129	195	242	283	352
	15	106	128	204	243	297	359
		Penetrating Ratio					
5	0	1.0	1.0	0.84	0.63	0.61	0.49
	15	1.0	1.0	0.81	0.62	0.61	0.50
7	0	0.85	0.64	0.58	0.45	0.50	0.38
	15	0.85	0.65	0.53	0.45	0.48	0.38
9	0	0.63	0.50	0.50	0.38	0.25	0.33
	15	0.61	0.51	0.46	0.38	0.43	0.30
		Efficiency Index (mm/s)					
5	0	12	31	46	55	72	73
	15	14	30	44	54	71	73
7	0	49	51	80	76	106	97
	15	46	51	74	76	99	96
9	0	66	64	98	91	71	114
	15	65	64	94	91	126	108

Table B5. Average Relative Velocity, Penetrating Ratio and Efficiency Index for The Quick-return Drive Center Distance h=25 mm

Freq. (Hz)	Mean Hanger Angle (deg.)	Amplitude (mm) 6, Screen Slope Angle (deg.) 5	6, 10	10, 5	10, 10	14, 5	14, 10
		Ave. Rel. Velocity (mm/s)					
5	0	9	22	42	57	89	99
	15	7	15	35	41	79	78
7	0	48	59	117	125	177	185
	15	44	47	105	104	159	152
9	0	93	101	171	184	242	253
	15	84	83	154	152	219	212
		Penetrating Ratio					
5	0	1.0	1.0	0.98	0.76	0.75	0.66
	15	1.0	1.0	1.0	0.87	0.80	0.71
7	0	1.0	0.75	0.65	0.58	0.60	0.53
	15	1.0	0.88	0.70	0.63	0.48	0.58
9	0	0.70	0.60	0.58	0.48	0.35	0.48
	15	0.78	0.68	0.45	0.53	0.30	0.53
		Efficiency Index (mm/s)					
5	0	9	22	41	43	67	65
	15	7	15	35	36	63	56
7	0	48	45	76	72	106	97
	15	44	42	74	65	76	87
9	0	65	60	98	87	85	120
	15	65	56	69	81	66	111

Table B6. Average Relative Velocity, Penetrating Ratio and Efficiency Index for The Quick-return Drive Center Distance h=40 mm

Freq. (Hz)	Mean Hanger Angle (deg.)	Amplitude (mm) 6, Screen Slope Angle (deg.) 5	6, 10	10, 5	10, 10	14, 5	14, 10
		Ave. Rel. Velocity (mm/s)					
5	0	8	23	44	59	95	104
	15	6	16	35	44	80	81
7	0	51	62	122	132	183	194
	15	42	48	108	105	164	159
9	0	94	104	175	190	249	267
	15	86	86	156	157	223	219
		Penetrating Ratio					
5	0	1.0	1.0	0.99	0.76	0.70	0.61
	15	1.0	1.0	1.0	0.87	0.79	0.70
7	0	1.0	0.74	0.64	0.55	0.47	0.49
	15	1.0	0.90	0.70	0.60	0.39	0.55
9	0	0.70	0.59	0.52	0.48	0.33	0.43
	15	0.77	0.66	0.43	0.53	0.28	0.48
		Efficiency Index (mm/s)					
5	0	8	23	43	44	66	63
	15	6	16	35	39	63	56
7	0	51	46	77	73	85	95
	15	42	43	76	63	64	88
9	0	66	61	91	90	81	114
	15	66	57	67	83	61	104